To assess the immunogenicity of rMPrP in mice, sera of immunized mice were subjected to ELISA to detect specific IgG antibodies against rMPrP. In the mice immunized with rMPrP, high antibody titers were detected (Fig. 1). The result indicates that rMPrP was highly immunogenic in BALB/c mice. No specific signal was detected in the sera from control animals that received only adjuvant with PBS.

To test the protective ability of the PrP-specific immunoglobulins, we intraperitoneally inoculated mouse brain homogenate of Obihiro strain into the immunized mice 7 weeks after the booster immunization, when antibody titer is highly elevated (Fig. 1). Non-immunized BALB/c mice ($n = 4$) developed the disease 318 ± 18.9 (AVE ± SD) days post-inoculation (p.i.), and the immunized mice succumbed to the disease at 308 ± 40.9 days p.i. The onset of disease was evaluated by clinical symptoms [20], and the deaths of prion disease were confirmed by detecting PrP^{Sc} in the brain by Western blot analysis. No significant difference in the incubation times could be detected statistically between the mice immunized with and without rMPrP, and incubation times of the immunized mice showed no correlation with anti-PrP antibody titers. Thus, our immunization procedure with rMPrP elicited high antibody titers, but had no prophylactic effect against the disease *in vivo*.

3.3. Interference of PrP^{Sc} replication in ScN2a-3 by antisera

To examine whether anti-PrP antibodies affect PrP^{Sc} formation in prion-affected cells, ScN2a-3 cells were incubated with sera from terminal-stage mouse scrapie, and PrP^{Sc} concentration was checked by Western blotting. We could not detect any inhibitory effects on PrP^{Sc} formation with the prion-affected mice sera (data not shown).

To examine whether anti-PrP antibodies induced by immunization inhibit PrP^{Sc} formation *in vitro*, we treated ScN2a-3 cells with immunized sera (Serum Nos. a–h) whose OD values of anti-PrP antibody in ELISA were highest (OD value; 0.92 ± 0.17) (Fig. 1). After the incubation with sera, ScN2a-3 cells were subjected to Western blotting for PrP^{Sc} detection. We detected stronger inhibition of PrP^{Sc} formation in four of eight rMPrP-immunized mice sera compared to non-immunized sera (Fig. 2). The mAb 31C6 on ScN2a-3 cells was used as positive control [21].

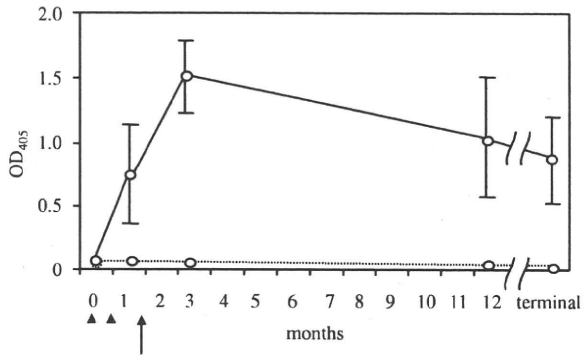

Fig. 1. Antibody response and incubation times in mice immunized with rMPrP and inoculated with Obihiro strain scrapie. Twenty mice were immunized with the rMPrP twice at 2-week intervals and anti-PrP IgG antibodies were detected in sera of the immunized mice by ELISA against rMPrP. Antibody responses in mice immunized with rMPrP. Sera from pre-immunization, 8, 16 and 43 weeks, and terminal stage were diluted to 1:100 and subjected to ELISA against purified rMPrP. The solid line and dotted line demonstrate sera from immunized with rMPrP and non-immunized mice, respectively. The arrowhead and arrow indicate the immunization/boost immunization and inoculation, respectively.

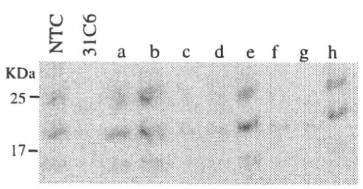

Fig. 2. Inhibition of PrP^{Sc} formation *in vitro*. Western blot analysis of ScN2a-3 exposed to immunized mice sera. Sera from eight individuals (Serum Nos. a–h) with higher antibody titers were used for assay. Normal mouse serum was added for negative control. The mAb 31C6 known to prohibit PrP^{Sc} formation was added as a control. Serum Nos. c, d, f and g showed inhibition of PrP^{Sc} formation. The molecular weights are shown in the left side. The experiment was repeated three times.

3.4. Epitope analysis of antibodies in sera

To determine epitopes recognized by antibodies in sera, Pepspot analysis was carried out (Fig. 3A and B). The epitopes determined from Pepspot analysis are shown in Fig. 3B. Antibodies reacted with various peptide spots. The terminal sera (Serum Nos. 1, 4 and 7 in Table 2) reacted with rMPrP in ELISA and broadly recognized peptide spots ranging from the C- to N-terminal. The terminal sera (Serum Nos. 4, 10 and 14 in Table 2) reacted with prion-affected brain homogenates in ELISA have a common epitope, TKGENF (aa 192–197). The rMPrP-immunized mouse sera reacted with several partial segments in the Pepspot residues. Six of eight sera strongly reacted with spot 88 and 89 corresponding to aa 158–169 (Serum Nos. a, c–e, g and h. Partially shown in Fig. 3A), and three of four sera with PrP^{Sc} formation-inhibiting effects reacted primarily with aa 142–153 (Serum Nos. c, d and f). This region contains tyrosine repeat motif YY (aa 148–153) [22,8], and the first α-helix of PrP (aa 144–154) [23], both important for PrP^{Sc} replication. Anti-PrP mAb 31C6 effectively inhibited PrP^{Sc} formation and recognized aa 143–151 [19] containing the first α-helix region of PrP. These regions also reacted with sera without inhibiting PrP^{Sc} formation (Serum Nos. a and b; shown in Fig. 3B), but the epitope was shorter than that of sera with inhibitory ability (Fig. 3B). Other reacted regions were aa 220–227 (Serum Nos. a and c), aa 201–210 (Serum No. a) and aa 140–171 (Serum Nos. b and f) (Fig. 3B).

4. Discussion

For many years, it was generally assumed that neither an inflammatory response nor an immune response was involved in the pathogenicity of prion diseases. Recently, PrP^{Sc} accumulation in lymphoid tissues before becoming detectable in the CNS [24] has been reported, and many studies have pointed to the role of the lymphoreticular cells in PrP^{Sc} accumulation, replication and transport from the peripheral lymphoid organs to the CNS [25,26]. Although the role of the immune system in prion diseases is controversial, the adaptive immune system appears unresponsive to prion infection because no production of anti-PrP antibodies is evident in the course of TSE infection [7].

In our experiment, antibodies against PrP were screened in sera from experimentally prion-infected mice. We tested prion-infected mice sera against mouse brain homogenate of mouse scrapie Obihiro strain and mouse brain homogenate of mouse-adapted BSE strain (Table 1B). Some sera reacted with rMPrP but not prion-infected brain homogenate, and *vice versa* (Table 2). We could not detect anti-PrP antibody titers in several mouse strains including NOD and A/J mice that possess autoimmune property. These results indicate that PrP molecules can be recognized as antigens by the host immune system under certain conditions. The OD value shown in Table 2 is low, however, we actually confirm the data at least six times by ELISA assay, and most of all sample repeated nine times assay. The cut-off value was set as AVE + 3SD that is high en-

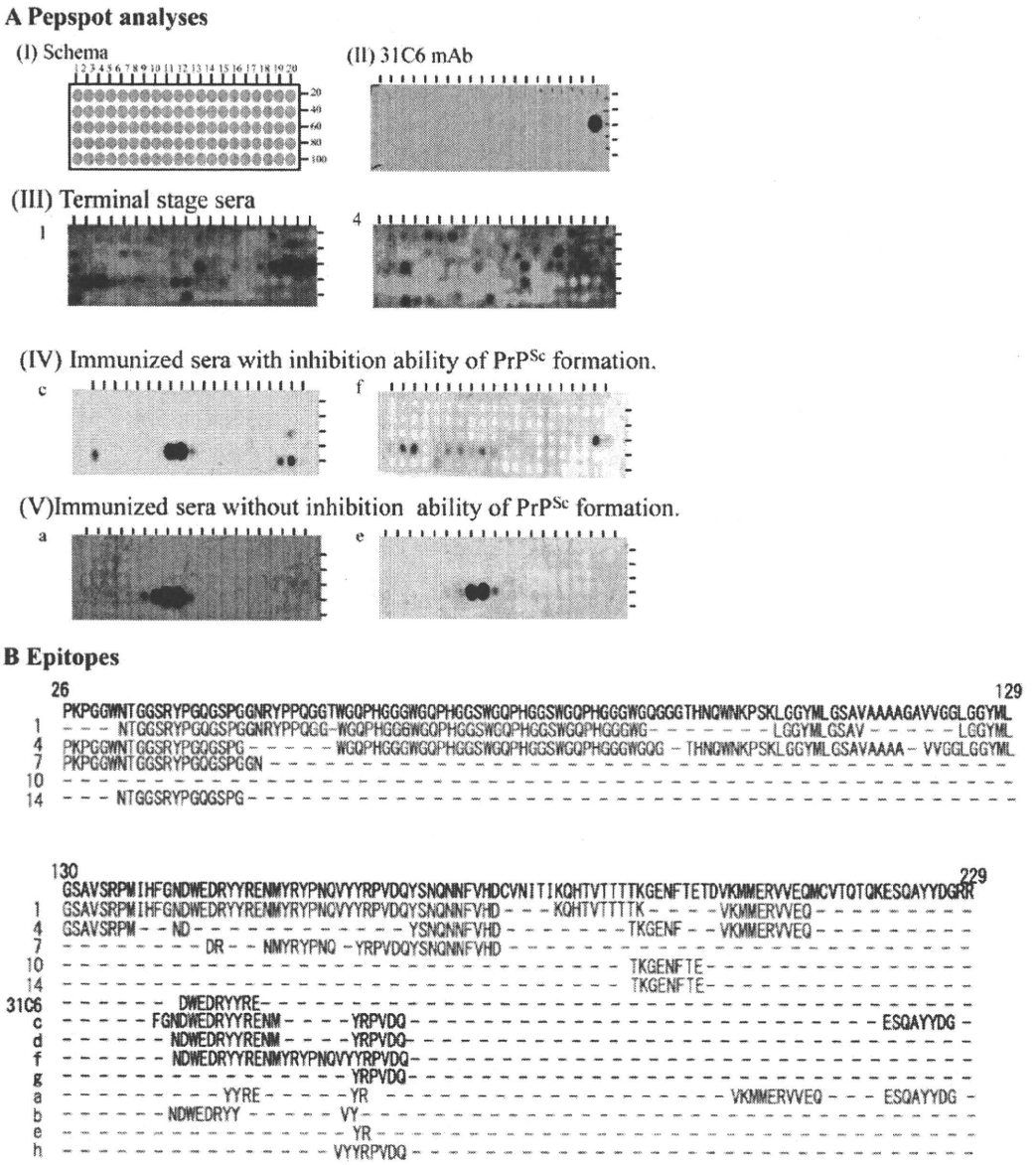

Fig. 3. Pepspot analyses of mice sera. Pepspot analyses of terminal stage and immunized mice sera. (A) Representative pictures of peptide spots are shown. Antibodies in each serum reacted with various peptide spots. Bars on the top and the right indicate the positions of the spots. (I) Schema of Pepspot membrane with spot numbers. (II) Pepspot membrane of 31C6 monoclonal antibody. (III) Pepspot membrane of terminal stage sera. Sera from five individuals (Serum Nos. 1, 4, 7, 10 and 14) with anti-PrP antibody titer were used for assay. Serum numbers correspond to those in Table 2. Pepspot membrane of immunized mice sera with (IV; Serum Nos. c, d, f and g) and without (V; Serum Nos. a, b, e and h) the ability to inhibit PrP^{Sc} formation. Serum numbers correspond to those of Fig. 2. (B) Epitopes recognized by mice sera. The epitopes of terminal stage mice sera (Serum Nos. 1, 4, 7, 10 and 14) are shown in black, and those of immunized sera with the ability to inhibit PrP^{Sc} formation (Serum Nos. c, d, f and g) and without the ability (Serum Nos. a, b, e and h) are shown in black characters and gray characters, respectively. The epitope of 31C6 mAb is also shown in black characters.

ough to eliminate false negative results. From Pepspot analysis shown in Fig. 3, the sera showed the reactivity against rMPrP. However, the result of Pepspot showed broadly recognizing region, hence we could not eliminate the possibility of cross-reaction.

Although they recognize the recombinant PrP against which they were raised, the antibodies often do not react with PrP^{C} or PrP^{Sc}, because of differences in the structure, molecular weight and purity of these antigens [27]. Moreover, some sera reacted with both prion-infected and uninfected mouse brain homogenates in our experiment (data not shown). This indicates that sera were not specific for PrP^{Sc}, because uninfected mouse brain homogenates contain PrP^{C} molecules. This is also supported by the data showing that sera did not react with purified PrP^{Sc} (Table 1A).

Pepspot analyses showed that some sera have epitope-covering peptides that are known to inhibit PrP^{Sc} formation. We retroactively compared the survival periods of mice with and without detectable anti-PrP antibodies; however, we could not find any correlation between anti-PrP antibodies and survival (data not shown). This is probably due to very low titers of the antibodies against the PrP in the sera, even though the signals were slightly detectable by ELISA. The antibodies in sera generated by inoculation could not have prophylactic effect because antibodies could not pass the blood–brain barrier.

We confirmed the immunogenicity of PrP by immunizing mice with rMPrP. BALB/c mice received conventional immunization of rMPrP with Freund's adjuvant, and developed high antibody titer

to rMPrP (Fig. 1). In Pepspot analysis, various peptide spots were detected by rMPrP-immunized mouse sera (Fig. 3A). Importantly, the mouse PrP aa 143–151 was detected in mice sera which interfered with PrP^{Sc} production. Anti-PrP antibodies recognizing the first α-helix region of PrP (aa 144–154) effectively inhibit PrP^{Sc} formation in cultured cells [23]. However, sera without PrP^{Sc}-inhibiting effects also bind with this region. There is the possibility that the sera mainly recognize conformational epitopes rather than sequential epitopes, although it is difficult to investigate conformational epitope because PrP^{Sc} conformation has not been fully determined. In our study, the serum from immunized mice containing antibodies recognized this region; however, the immunization of mice with rMPrP elicited no prophylactic effect against Obihiro strain mouse scrapie, even though mice developed high titers of anti-PrP antibody. It is reported that the 31C6 mAb generated by PrP^{C} immunization in PrP^{C} knockout mouse, recognizes liner epitope, and inhibit PrP^{Sc} formation *in vitro*, showing prophylactic effect *in vivo* [28]. Therefore, the anti-PrP antibody recognizing liner epitope could neutralize PrP^{Sc} and prolong incubation periods. Though the mechanism of antibody-mediated interference has been obscure, it has generally been considered that anti-PrP antibodies may mask PrP^{C} sites critical for PrP^{Sc} replication. However, anti-PrP antibody is generated in wild-type mice in our study, hence the property is different from 31C6 mAb that is generated in the PrP^{C} knockout mouse.

Several reports that showed prolongation of the disease course with PrP immunization emphasize strong immunization protocols [14,15,29]. Although repeated injections of CFA [30] into mice delayed the onset of the clinical disease even in the absence of PrP immune response, combination with PrP and CFA prolongs longer. Therefore, immunization with PrP might have a prophylactic effect. In our study, we immunized mice with rMPrP and Freund's adjuvant in order to investigate the prophylactic effect of PrP itself. Although the anti-PrP antibody does not possess strong prophylactic effect *in vivo*, it may be able to prolong the onset of prion disease when the prion dose is very low. The reason why we could not show a prophylactic effect of anti-PrP antibodies *in vivo* may be related to the fact that the administered prion dose was greater than the amount that could be prevented by the antibody or, alternatively, that the prion administered by the i.p. route could directly contact the lymph reticular system or nerves before being saturated by antibody. The presence of anti-PrP antibody may cause a difference *in vivo* when prion is administered at a low dose and by the oral route.

Our experiments focused on anti-PrP IgG antibody; however, the relationship between prion disease and anti-PrP antibodies is undoubtedly more complicated in naturally infected animals. Recent studies reported that secretory immunoglobulin A (sIgA) elicited by mucosal immunization attenuated orally acquired TSE in mice [31]. The agent could be taken up from the intestines in the natural infection, meaning that not only serum IgG but also sIgA may play important roles in preventing the progression of the disease. The sIgA could sequester part of the administered prions by binding and neutralizing the pathogen itself. The sIgA–prion complex may be difficult to take up *in vivo*, or even after being taken up, it may hinder the conversion of PrP^{C} to PrP^{Sc}. Therefore, the anti-PrP sIgA may play an important role, especially at the prion uptake stage. Investigating local immunity such as gut immunity may be important for understanding prion disease progression in the body.

Acknowledgments

We thank Dr. Motohiro Horiuchi (Hokkaido University, Japan) for providing mAbs 31C6 and 44B1 and N2a-3 cell. This work was supported in part by grants from the Ministry of Education, Culture, Sports, Science and Technology (Project Code; 0000175104) and from the Ministry of Health, Labour and Welfare, Japan.

References

[1] S.B. Prusiner, Prions, Proc. Natl. Acad. Sci. USA 95 (1998) 13363–13383.
[2] B. Caughey, G.J. Raymond, The scrapie-associated form of PrP is made form a cell surface precursor that is both protease- and phospholipase-sensitive, J. Biol. Chem. 266 (1991) 18217–18223.
[3] A.C. Gardiner, Gel diffusion reactions of tissues and sera from scrapie-affected animals, Res. Vet. Sci. 7 (1966) 190–195.
[4] M.C. Clarke, D.A. Haig, Attempts to demonstrate neutralizing antibodies in the sera of scrapie-affected animals, Vet. Rec. 78 (1966) 647–649.
[5] P. Brown, J. Hooks, R. Roos, D.C. Gajdusek, C.J. Gibbs Jr., Attempt to identify the agent for Creutzfeldt-Jakob disease by CF antibody relationship to known viruses, Nat. New Biol. 235 (1972) 149–152.
[6] R.F. Marsh, I.C. Pan, R.P. Hanson, Failure to demonstrate specific antibody in transmissible mink encephalopathy, Infect. Immun. 2 (1970) 727–730.
[7] D.D. Porter, H.G. Porter, N.A. Cox, Failure to demonstrate a humoral immune response to scrapie infection in mice, J. Immunol. 111 (1973) 1407–1410.
[8] V. Curin Serbec, M. Bresjanac, M. Popvic, K. Pretnar Hartman, V. Galvani, R. Rupreht, M. Cernilec, T. Vranac, I. Hafner, R. Jerala, Monoclonal antibody against a peptide of human prion protein discriminates between Creutzfeldt-Jacob's disease-affected and normal brain tissue, J. Biol. Chem. 279 (2004) 3694–3698.
[9] S.C. Collis, R.H. Kimberlin, G.C. Millson, Immunoglobulin G concentrations in the sera of Herdwick sheep with natural scrapie, J. Comp. Pathol. 89 (1979) 389–396.
[10] S. Betmouni, V.H. Perry, J.L. Gordon, Evidence for an early inflammatory response in the central nervous system of mice with scrapie, Neuroscience 74 (1996) 1–5.
[11] R.J. Kascsak, R. Rubenstein, P.A. Merz, M. Tonna-DeMasi, R. Fersko, R.I. Carp, H.M. Wisniewski, H. Diringer, Mouse polyclonal and monoclonal antibody to scrapie-associated fibril proteins, J. Virol. 61 (1987) 3688–3693.
[12] R. Rubenstein, R.J. Kascsak, M. Papini, R. Kascsak, R.I. Carp, G. LaFauci, R. Meloen, J. Langeveld, Immune surveillance and antigen conformation determines humoral immune response to the prion protein immunogen, J. Neurovirol. 5 (1999) 401–413.
[13] L. Souan, Y. Tal, Y. Felling, I.R. Cohen, A. Taraboulos, F. Mor, Modulation of proteinase-K resistant prion protein by prion peptide immunization, Eur. J. Immunol. 31 (2001) 2338–2346.
[14] E.M. Sigurdsson, E.R. Brown, M. Daniels, R.J. Kascsak, R. Kascsak, R. Carp, H.C. Meeker, B. Frangione, T. Wisniewski, Immunization delays the onset of prion disease in mice, Am. J. Pathol. 161 (2002) 13–17.
[15] A. Schwarz, O. Kratke, M. Burwinkel, C. Riemer, J. Schultz, P. Henklein, T. Bamme, M. Baier, Immunisation with a synthetic prion protein-derived peptide prolongs survival times of mice orally exposed to the scrapie agent, Neurosci. Lett. 350 (2003) 187–189.
[16] A.R. White, P. Enever, M. Tayebi, R. Mushens, J. Linehan, S. Brandner, D. Anstee, J. Collinge, S. Hawke, Monoclonal antibodies inhibit prion replication and delay the development of prion disease, Nature 422 (2003) 80–83.
[17] D.C. Bolton, P.E. Bendheim, A.D. Marmorstein, A. Potempska, Isolation and structural studies of the intact scrapie agent protein, Arch. Biochem. Biophys. 258 (1987) 579–590.
[18] M. Shinagawa, K. Takahashi, S. Sasaki, S. Doi, H. Goto, G. Sato, Characterization of scrapie agent isolated from sheep in Japan, Microbiol. Immunol. 29 (1985) 543–551.
[19] C.L. Kim, A. Umetani, T. Matsui, N. Ishiguro, M. Shinagawa, M. Horiuchi, Antigenic characterization of an abnormal isoform of prion protein using a new diverse panel of monoclonal antibodies, Virology 320 (2004) 40–51.
[20] A.G. Dikinson, V.M. Meikle, A comparison of some biological characteristics of the mouse-passaged scrapie agents, 22A and ME7, Genet. Res. 13 (1969) 213–215.
[21] C.L. Kim, A. Karino, N. Ishiguro, M. Shinagawa, M. Sato, M. Horiuchi, Cell-surface retention of PrP^{C} by anti-PrP antibody prevents protease-resistant PrP formation, J. Gen. Virol. 85 (2004) 3473–3482.
[22] E. Paramithiotis, M. Pinard, T. Lawton, A prion protein epitope selective for the pathologically misfolded conformation, Nat. Med. 9 (2003) 893–899.
[23] D. Peretz, R.A. Williamson, K. Kaneko, J. Vergara, E. Leclerc, G. Schmitt-Ulms, I.R. Mehlhorn, G. Legname, M.R. Wormald, P.M. Rudd, R.A. Dwek, D.R. Burton, S.B. Prusiner, Antibodies inhibit prion propagation and clear cell cultures of prion infectivity, Nature 412 (2001) 739–743.
[24] R.A. Somerville, C.R. Birkett, C.F. Farquhar, N. Hunter, W. Goldmann, J. Dornan, D. Grover, R.M. Hennion, C. Percy, J. Foster, M. Jeffrey, Immunodetection of PrP^{Sc} in spleens of some scrapie-infected sheep but not BSE-infected cows, J. Gen. Virol. 78 (1997) 2389–2396.
[25] M.A. Klein, R. Frigg, E. Flechisig, A.J. Raeber, U. Kalinke, H. Bluethmann, F. Bootz, M. Suter, R.M. Zinkernagel, A. Aguzzi, A crucial role for B cells in neuroinvasive scrapie, Nature 390 (1997) 687–690.
[26] F. Montrasio, R. Frigg, M. Glatzel, M.A. Klein, F. Mackay, A. Aguzzi, C. Weissmann, Impaired prion replication in spleens of mice lacking functional follicular dendritic cells, Science 288 (2000) 1257–1259.

[27] F.L. Heppner, A. Aguzzi, Recent developments in prion immunotherapy, Curr. Opin. Immunol. 16 (2004) 594–598.
[28] C.H. Song, H. Furuoka, C.L. Kim, M. Ogino, A. Suzuki, R. Hasebe, M. Horiuchi, Effect of intraventricular infusion of anti-prion protein monoclonal antibodies on disease progression in prion-infected mice, J. Gen. Virol. 89 (2008) 1533–1544.
[29] M. Polymenidou, F.L. Heppner, E.C. Pellicioli, E. Urich, G. Miele, F. Wopfner, H.M. Schaetzl, B. Becher, A. Aguzzi, Humoral immune response to native eukaryotic prion protein correlates with anti-prion protection, Proc. Natl. Acad. Sci. USA 101 (2004) 14670–14676.
[30] Y. Tal, L. Souan, I.R. Cohen, A. Meiner, A. Taraboulos, F. Mor, Complete Freund's adjuvant immunization prolongs survival in experimental prion disease in mice, J. Neurosci. Res. 71 (2003) 286–290.
[31] S. Bade, M. Baier, T. Boetel, A. Frey, Intranasal immunization of Balb/c mice against prion protein attenuates orally acquired transmissible spongiform encephalopathy, Vaccine 24 (2006) 1242–1253.

Veterinary Immunology and Immunopathology 133 (2010) 33–39

Contents lists available at ScienceDirect

Veterinary Immunology and Immunopathology

journal homepage: www.elsevier.com/locate/vetimm

Research paper

Bovine macrophage degradation of scrapie and BSE PrP^{Sc}

Yukiko Sassa, Yasuo Inoshima, Naotaka Ishiguro *

Laboratory of Food and Environmental Hygiene, Department of Veterinary Medicine, Faculty of Applied Biological Sciences, Gifu University, 1-1 Yanagido, Gifu-city, Gifu, 501-1193, Japan

ARTICLE INFO

Article history:
Received 9 February 2009
Received in revised form 15 May 2009
Accepted 29 June 2009

Keywords:
BSE
Bovine
Degradation
Macrophage
PrP^{Sc}

ABSTRACT

Transmissible spongiform encephalopathies (TSEs), such as bovine spongiform encephalopathy (BSE) and scrapie, display long incubation periods before PrP^{Sc} accumulates in the central neuronal system (CNS). The precise role that phagocytic cells, such as macrophages, play in prion pathogenesis is uncertain. In this study, the involvement of bovine macrophages at the early stage of prion infection was studied. Brain homogenates of mouse scrapie and BSE were degraded sequentially in the bovine macrophage cell line, Bo120, and freshly prepared in monocyte-derived macrophages from peripheral blood. Mouse scrapie brain homogenates degraded in Bo120 cells were inoculated intraperitoneally to C57BL mice, showing that the degree of cellular degradation (2 h, 10, 28, and 36 d) correlated with survival periods (288, 303, 324, and 340 d, respectively). Partial colocalizations of PrP and lysosomes were observed in Bo120 cells by confocal microscopy. These results suggest that bovine macrophages have the ability to take up and degrade PrP^{Sc}, resulting in decreased TSE infectivity in mice.

1. Introduction

Transmissible spongiform encephalopathies (TSEs) are progressive neurodegenerative diseases caused by pathogenic isoforms (PrP^{Sc}) of host-encoded cellular prion proteins (PrP^{C}). PrP^{Sc} are β-sheet enriched structures that are partially resistant to proteinase K (PK). TSEs include scrapie in sheep and goats, bovine spongiform encephalopathy (BSE) in cattle, chronic wasting disease (CWD) in deer and elk, and Creutzfeldt-Jakob disease (CJD) in humans. The appearance of a variant CJD (vCJD) has raised public health concerns that BSE might be transmissible to humans across the species barrier by dietary exposure of BSE-contaminated foodstuffs (Collinge et al., 1996).

TSEs invasion sites are controversial; but natural infection may occur orally, especially through the gut. The route of TSE invasion from the gut to CNS still remains unclear. Previous reports showed that immune cells participate in the pathogenesis of murine TSEs (Montrasio et al., 2000; Mabbott et al., 2000). Following an oral inoculation using a mouse scrapie and BSE model, PrP^{Sc} was detected in the spleen and lymph reticular system (LRS) before reaching the CNS (Maignien et al., 1999). This finding indicates PrP^{Sc} replicates primarily in immune cells, and suggests that the immune system is involved in either PrP^{Sc} propagation or transmission to the CNS.

BSE pathogenesis in bovine differs from TSEs of other species in terms of infectivity distribution. In cattle, no infectivity is seen in LRS except in the distal ileum (Buschmann and Groschup, 2005) and tonsils (Wells et al., 2005). In other species, however, strong infectivity is found in LRS (van Keulen et al., 1996; Sigurdson et al., 2002). These species-specific variations are possibly the reflection of their respective TSE pathogenesis and host clearance systems. Although host responses have mainly been studied using the murine scrapie model, BSE pathogenesis in cattle differs from mice as described above. A host response study using a cattle host is urgently needed in order to understand BSE.

BSE has been diagnosed in 180,000 cattle in the U.K. (Anderson et al., 1996) affecting approximately 0.1%

* Corresponding author. Tel.: +81 58 293 2864; fax: +81 58 293 2864.
E-mail address: ishiguna@gifu-u.ac.jp (N. Ishiguro).

0165-2427/$ – see front matter © 2009 Elsevier B.V. All rights reserved.
doi:10.1016/j.vetimm.2009.06.018

(Department for Environment, Food and Rural Affairs, UK, http://www.defra.gov.uk/animalh/bse/controls-eradication/feedban-bornafterban.html). It is thought that oral administration of PrP^{Sc}-contaminated MBM is the cause for a worldwide epidemic. Although most cows are fed with a PrP^{Sc}-contaminated MBM, most are not diagnosed with BSE. We suggest that the bovine immune system serves as one potential PrP^{Sc} clearance system because macrophages generally act as a host defense mechanism against exogenous pathogen. On the other hand, the PrP^{Sc} contained bovine immune cells could move inside the body so that they could contact with nerve ending. Bovine immune cells possibly act not only as a propagation system, but also a PrP^{Sc} clearance system.

Here, we studied the role of bovine macrophage as the initial host responder in early stage prion infection. Mouse scrapie and BSE brain homogenates were degraded in macrophages *in vitro*. Mice inoculated with the degraded intracellular PrP^{Sc} showed decreased infectivity. Partial colocalizations of PrP and lysosomes were then observed in cells by confocal microscopy.

2. Materials and methods

2.1. Cell cultures and media

Bo120 cells were generated from a cultured bovine macrophage strain spontaneously established from bovine peripheral blood. Monocyte-derived macrophages were mainly macrophages freshly collected from bovine peripheral monocytes purified by Ficoll-Conray density gradient centrifugation before adherence to plastic. Bo120 cell line and the monocyte-derived macrophages were maintained in Dulbecco's MEM (DMEM; Sigma, St Louis, MO, USA) and RPMI1640 (Sigma) supplemented with 10% inactivated fetal calf serum (FCS), 10,000 units/ml of streptomycin and penicillin, and 2.5 μg/ml of amphotericin B, respectively.

2.2. Cellular uptake

Cells were incubated with 1% mouse scrapie brain homogenate or FITC-latex particles (1 μm diameter, Polysciences, Inc.; Warrington, PA, USA) for 8 h at 37 or 4 °C. The cells were fixed with cold methanol and then incubated with mAb 31C6 (Kim et al., 2004a) for PrP detection following incubation with anti-mouse alexa488 (Invitrogen, Carlsbad, CA, USA). The slides were then analyzed using a fluorescence microscope (Nikon, Tokyo, Japan).

2.3. Flow cytometry analyses

Cells were labeled with different monoclonal antibodies (mAbs): mouse anti-equine MHC class II (clone number, CVS20), anti-MHC class I (PT85A), mouse anti-ovine CD14 (VPM65), mouse anti-bovine CD11b (CC126), anti-ovine CD11c (BAQ153A), anti-PrP (6H4), and appropriate Ig isotype controls (DakoCytomation, Glostrup, Denmark). All mAbs were purchased from Serotec (Oxford, UK) with the exception of anti-MHC class I and CD11c (VMRD; Pullman, WA, USA), and anti-PrP (Prionics, Zurich, Switzerland). Fluorescence isothiocyanate (FITC)-conjugated anti-mouse antibody (ICN Pharmaceuticals, Costa Mesa, CA, USA) was used as the secondary antibody, and propidium iodide (Sigma) was used to identify dead cells. Cells were analyzed with CellQuestPro software on a FACSCalibur flow cytometer (BD Biosciences, San Jose, CA, USA).

2.4. Macrophage uptake and degradation experiments

Brain homogenates of mouse scrapie and BSE were prepared with PBS from the terminal stage of mice inoculated with mouse scrapie Obihiro strain (Shinagawa et al., 1986) and Kanagawa case no. 10 (http://www.maff.go.jp/index.html), respectively. Brain homogenates of 0.01% (w/v) mouse scrapie brain or 0.1% BSE brain were added to cells, following media removal, cell wash, and cell culture until collection. Lipopolysaccharide (LPS) (Sigma) was used at a final concentration of 1 μg/ml. The toxic effects of brain homogenates on cell cultures were analyzed using the lactate dehydrogenase (LDH) release assay and LDH-cytotoxic test (Sigma). The cells were collected with supernatant in order to prevent loss of PrP^{Sc} from culture media. The collected supernatant and cells were centrifuged at 2150 × *g* for 10 min, and pellets were dissolved in SDS–PAGE sample buffer. The PK digestion was performed as previously described (Kim et al., 2004b) with modification. The samples were then incubated with 0.3% sodium phosphotungstic acid (Wadsworth et al., 2001) before PK digestion and PK digested samples were centrifuged at 15,500 × *g* for 30 min instead of ultracentrifugation.

2.5. Western blot analysis

The samples were separated in 12% SDS–polyacrylamide gel and electroblotted onto PVDF membranes (Milipore, Billerica, MS, USA). They were then incubated with an anti-PrP mAb 31C6 and a polyclonal antibody B103 (Fujirebio, Tokyo, Japan) followed by peroxidase-conjugated anti-mouse or anti-rabbit antibodies (GE Healthcare, Waukesha, WI, USA). Immunodetection was visualized by enhanced chemiluminescence (ECL kit; GE Healthcare) and quantified with a LAS-4000 lumino image analyzer (Fujifilm, Tokyo, Japan).

2.6. Mouse bioassay

Bo120 cells were incubated with 0.01% mouse scrapie brain homogenate for 2 h. Once the media was removed, the cells were washed and cultured until collection. The collected samples were resuspended in 1 ml of PBS, and injected intraperitoneally (100 μl) into 4-week-old female C57BL/6 mice ($n = 6$). PBS was injected as a control ($n = 2$). Animals were examined daily for clinical signs until the terminal stage of their disease. The diagnosis of mouse scrapie was confirmed by PrP^{Sc} detection in brains after PK digestion using western blot analysis.

2.7. Laser scanning confocal microscopy analyses

Bo120 cells were incubated with 0.01% mouse scrapie brain homogenate for 2 h following media removal and cell

wash, and then cultured. LysoTracker DND99 (Invitrogen) was added to the culture for 2 h before fixation with 4% paraformaldehyde. The slides were post-fixed with cold methanol and incubated with mAb 31C6 following incubation with anti-mouse alexa488. The slides were analyzed using an LSM510 confocal microscope (Carl Zeiss, Oberkochen, Germany).

2.8. Statistical analyses

Statistical analyses were performed using the software package, ystat2006. Differences in survival periods between mice injected with material from different sources were compared using the Bonferroni test.

3. Results

3.1. Cell characterizations

To characterize cellular properties, aspects of latex particle and mouse scrapie brain homogenate uptake abilities along with the expression of cell surface antigens, were investigated in Bo120 cells and monocyte-derived macrophages. Both cell types actively took up FITC-latex

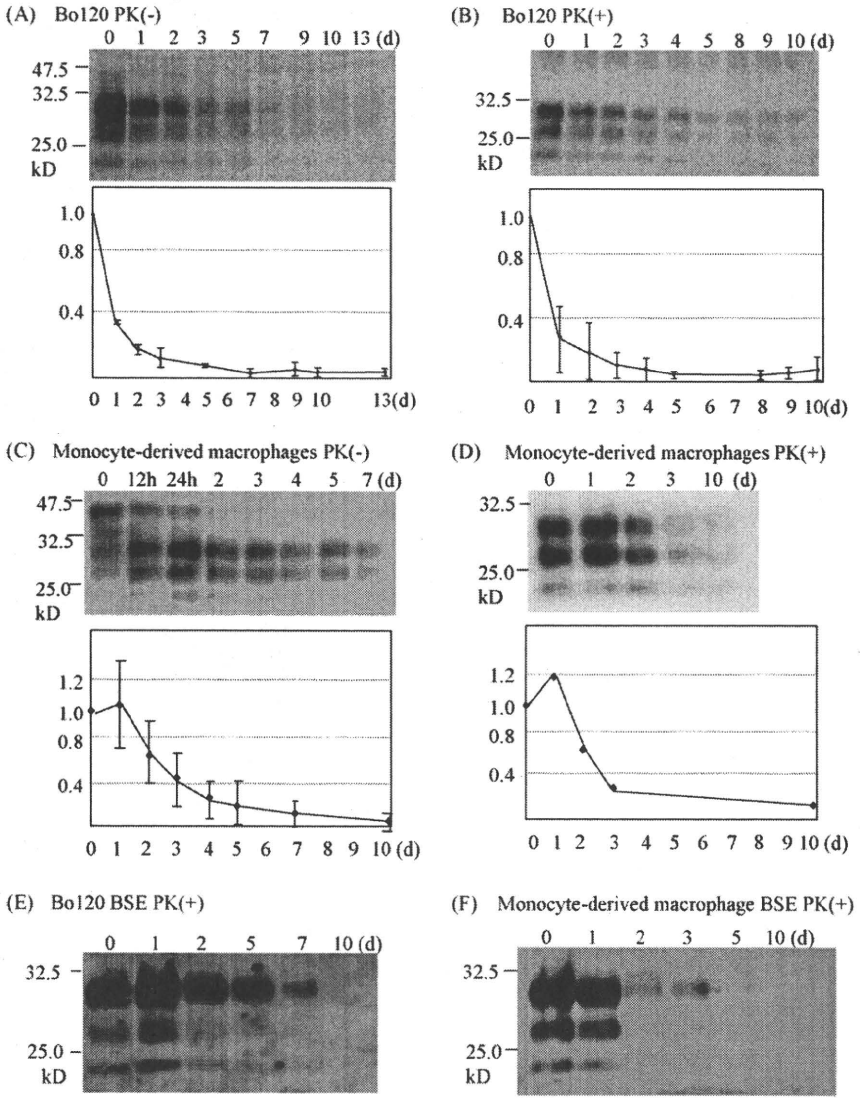

Fig. 1. Uptake and degradation of PrP^{Sc} by Bo120 cells and monocyte-derived macrophages. TSE affected brain homogenates were prominently degraded in both Bo120 and monocyte-derived macrophages. Western blots show the relative degradation of PrP^{Sc} in scrapie mouse brain homogenates in Bo120 cells without (A) and with (B) PK digestion, as well as in monocyte-derived macrophages without (C) and with (D) PK digestion. Western blots of BSE with PK digestion in Bo120 (E) and monocyte-derived macrophages (F) are shown. The PrP^{Sc} and PrP^{C} in 0.01% mouse scrapie brain homogenate in Bo120 cells was detected by mAb 31C6, and those in 0.1% BSE brain homogenate were detected by polyclonal antibody B103. The cells were incubated with mouse scrapie or BSE brain homogenates for the indicated times (0–13 d). The relative degradation of PrP^{Sc} and PrP^{C} in TSE-affected brain homogenates was quantified from 3 independent experiments, except (D) which was quantified from one. Day 0 is shown as a ratio of 1. Error bars show mean ± SD. BSE samples (E, F) were detected with X-ray films due to the sensitivity limitation of the LAS-4000 system.

particles and PrP^{Sc} in mouse scrapie brain homogenates. Introduction of FITC-latex particles or mouse scrapie brain homogenates in macrophages allowed fluorescence visualization at 37 °C. In contrast, there was no fluorescence of FITC-latex particles or PrP^{Sc} at 4 °C (data not shown). Surface antigens of Bo120 cells and monocyte-derived macrophages were analyzed by flow cytometry. Strong expression of MHC class I and PrP^{C}, and weak expression of CD14 were observed in Bo120 cells, while strong expression of MHC class II, CD14, CD11b and CD11c were seen in monocyte-derived macrophages (data not shown). LPS stimulation had no influence on these antigens in both Bo120 cells and monocyte-derived macrophages. Monocyte-derived macrophages expressed the CD14 antigen strongly, and both cells possessed phagocytic abilities, confirming the presence of macrophages.

3.2. Degradation of PrP^{Sc} in macrophages

In order to evaluate the degrading ability of bovine macrophages against PrP^{C} and PrP^{Sc}, mouse scrapie brain homogenate or BSE brain homogenate was added to the cells. Intracellular PrP^{Sc} were detected by western blot analysis after incubation periods of 2 h to 10 d. Anti-PrP mAb 31C6, which recognizes mouse PrP but not bovine PrP, was used to detect mouse scrapie brain homogenate. Alternatively, polyclonal antibody B103 was used to detect BSE brain homogenate. Bo120 cells (Fig. 1A) and monocyte-derived macrophages (Fig. 1C) phagocytosed and degraded PrP^{C} and PrP^{Sc} within mouse scrapie brain homogenate in a time-dependent manner. Western blot analysis indicated a 10-fold decrease after 10 d compared to 2 h. Reduction of mouse scrapie PrP^{Sc} was also confirmed by PK digested samples in Bo120 cells (Fig. 1B) and monocyte-derived macrophages (Fig. 1D). Bo120 cells (Fig. 1E) and monocyte-derived macrophages (Fig. 1F) degraded PrP^{Sc} within BSE brain homogenates. The PrP^{C} in bovine brain homogenates was eliminated by PK digestion. In Bo120 cells, the degradation of PrP^{C} and PrP^{Sc} within mouse scrapie brain homogenates was slower than that of PrP^{C} within normal mouse brain homogenates (data not shown). LPS activation of Bo120 cells prior to the addition of mouse scrapie brain homogenate did not affect degradation. In contrast, the LPS activation of monocyte-derived macrophages accelerated PrP^{C} and PrP^{Sc} breakdown (Fig. 2). The influence of mouse scrapie or BSE brain homogenates on cell toxicity was not observed by a LDH release assay, even with long-term treatment (10 d; data not shown).

3.3. Mouse bioassay of degraded products in Bo120 cells

The degraded products of mouse scrapie brain homogenates in Bo120 cells were intraperitoneally administered to C57BL mice in order to determine infectivity. Mouse inoculation samples were collected at 2 h, and 1, 3, 5, 8, 10, 18, 22, 28 and 36 d following the addition of mouse scrapie brain homogenates onto Bo120 cells, and then subjected to western blot analysis (Fig. 3A). The samples harvested at 2 h, and 10, 28 and 36 d were used as inocula for the mouse inoculation assay. All C57BL mice administered with the

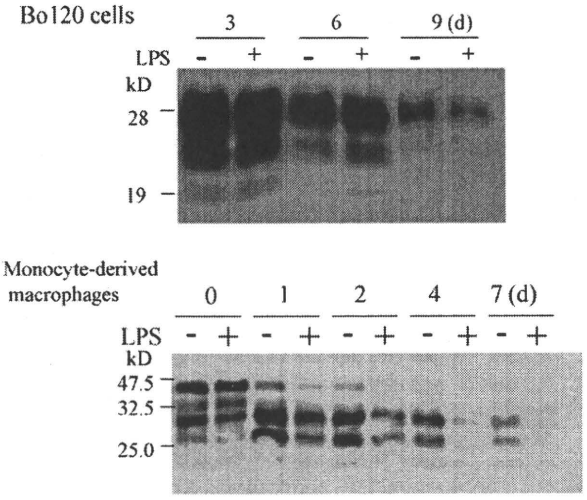

Fig. 2. Effect of LPS on the degradation of PrP^{C} and PrP^{Sc}. Bo120 (upper panel) and monocyte-derived macrophages (bottom panel) were exposed to mouse scrapie brain homogenates for days, as indicated with (+) or without (−) LPS-treatment.

inocula developed a progressive clinical disease with the exception of 1 mouse that lived with no clinical signs for over 700 d following inoculation. The survival period in clinically affected mice ranged from 288 to 384 d. The mean incubation period for mouse deterioration followed the Bo120 cell culture period. The murine groups injected with inocula from 2 h, and 10, 28 and 36 d died at 308 ± 16.1 d (mean incubation period ± SD), 324.5 ± 10.7, 332.0 ± 25.4, and 348.0 ± 11.5, respectively. The incubation time until development of terminal scrapie sickness is illustrated in Fig. 3B. Significant differences were found

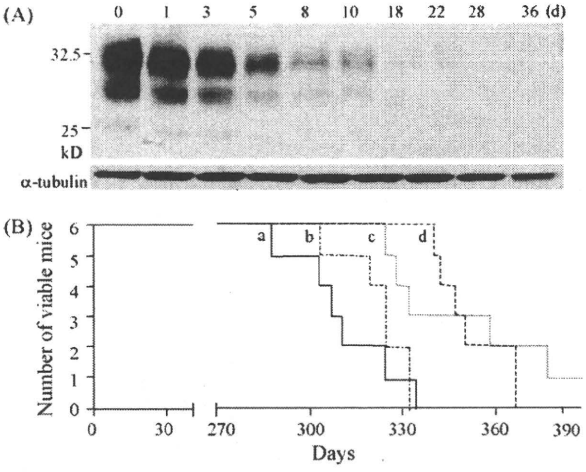

Fig. 3. Murine survival period following inoculation of mouse scrapie brain homogenates degraded by Bo120 cells. (A) Western blots show the degradation of PrP^{C} and PrP^{Sc} in mouse scrapie brain homogenates in Bo120 cells. Bo120 cells were cultured for the periods indicated after incubation with mouse scrapie brain homogenate. (B) Survival periods were monitored in female C57BL mice intraperitoneally inoculated with mouse scrapie brain homogenate degraded in Bo120 cells for: (a) 0 d; (b) 10 d; (c) 28 d; (d) 36 d. All mice were tested for PrP^{Sc} accumulation in the brain by western blot analysis. Survival periods were recorded until 390 d post-infection.

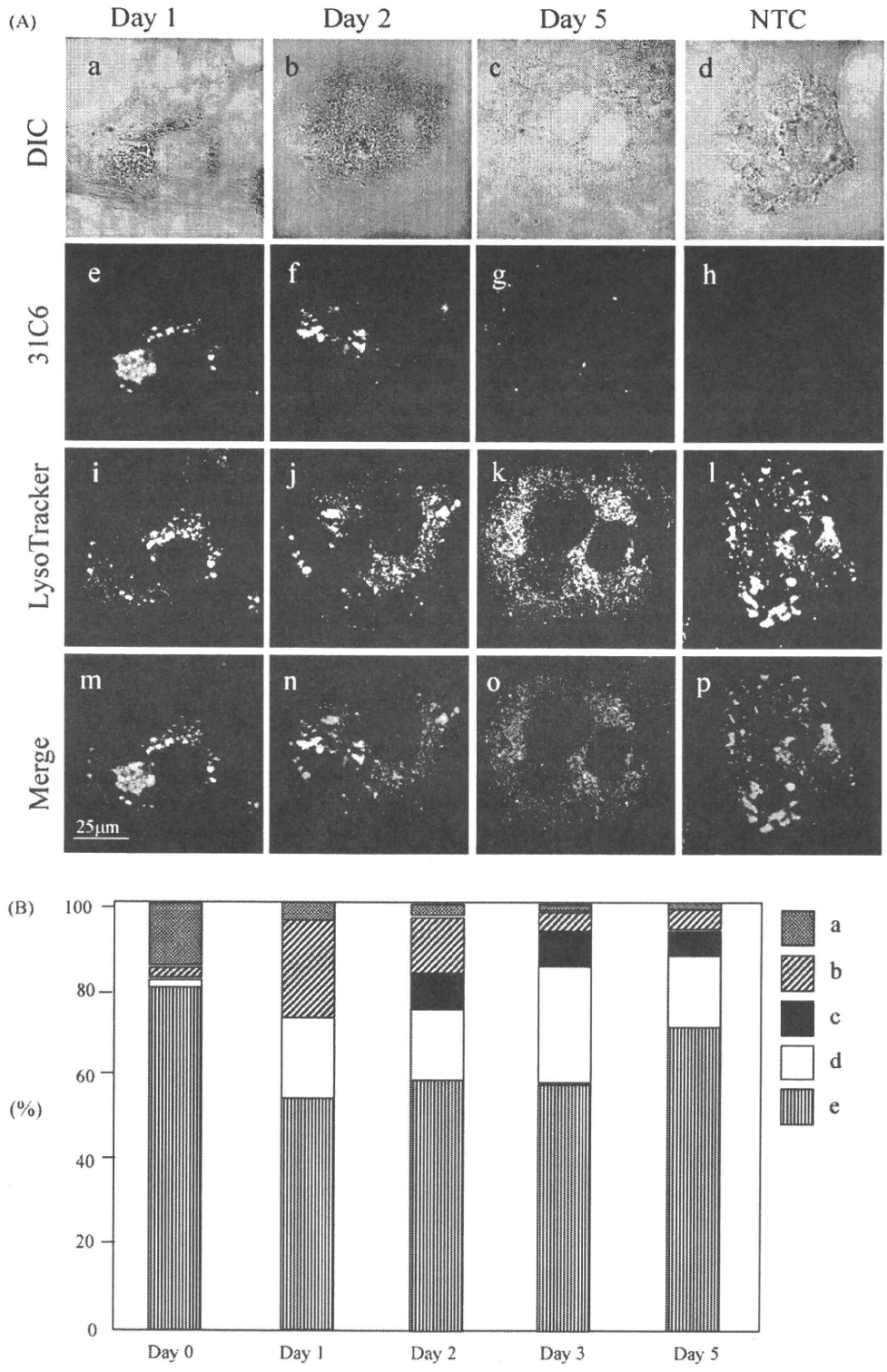

Fig. 4. (A) Colocalization of PrP^{C} and PrP^{Sc} in mouse scrapie brain homogenates with lysosomes in Bo120 cell macrophages. Bo120 cells were incubated with mouse scrapie brain homogenate for 1 d (a, e, i, and m), 2 d (b, f, j, and n) and 5 d (c, g, k, and o). The cells reacted with mAb 31C6 (e, f, and g) and LysoTracker fluorescence (i, j, k, and l). Negative control (NTC; d, h, l, and p) was inoculated with mouse scrapie brain homogenate for 2 d and detected by isotype control Ab instead of 132 mAb. A merged image of the green and red channels show partial colocalizations of PrP and lysosomes, and the yellow channels show colocalizations (m, n, o, and p). (B) A diagram of PrP^{C} and PrP^{Sc} degradation in mouse scrapie brain homogenate by Bo120 cells is shown. A total of 250 fields were counted and quantified for the relative degradation of PrP^{C} and PrP^{Sc} particles. (a) Large PrP^{C} and PrP^{Sc} particles on cell surface. (b) Big PrP^{C} and PrP^{Sc} aggregates in the cell. (c) Small PrP^{C} and PrP^{Sc} particles aggregated in the cell. (d) Small PrP^{C} and PrP^{Sc} particles in the cell. (e) No PrP^{C} and PrP^{Sc} in the cell. (For interpretation of the references to colour in this figure legend, the reader is referred to the web version of the article.)

between groups injected with inoculums at 2 h, as well as at 28 and 36 d. Our results indicate a correlation between the degradation of PrP^C and PrP^{Sc} *in vitro* and reduced prion infectivity *in vivo*, suggesting macrophage degradation reduces the infectivity of the scrapie prion. Diagnosis was confirmed for all clinically prion-affected mice through western blot analysis of brain extracts, and PrP^{Sc} accumulation levels were approximately the same among all 4 groups (data not shown).

3.4. Colocalizations of PrP and lysosome in Bo120 cells

To further confirm the degradation of PrP^C and PrP^{Sc} in macrophages, degradation of PrP^C and PrP^{Sc} in Bo120 cells was visualized directly via fluorescence confocal laser microscopy. On day 0, brain homogenate containing PrP was attached around the cell surface. On day 1, massive intracellular brain homogenates were observed. On day 2, a small gathering of PrP^C and PrP^{Sc} was present, representing a subdivision of small scrapie homogenates. On day 3, the small scrapie homogenates decreased and the large mass diminished. On day 5, PrP^C and PrP^{Sc} were barely detectable (Fig. 4A). Fluorescence cells were quantified by counting 250 fields. We found direct evidence of PrP^C and PrP^{Sc} degradation, i.e., macrophages broke PrP^C and PrP^{Sc} into small pieces within the cells. The large PrP^C and PrP^{Sc} particles on the cell surface were prominent on day 0. These large PrP^C and PrP^{Sc} particles were broken into small PrP^C and PrP^{Sc} particles continually from day 0 (Fig. 4B).

PrP^C and PrP^{Sc} localizations were investigated in order to determine the degradation pathways. We used aldehyde fixable LysoTracker red to visualize lysosomes and mAb 31C6 to detect scrapie mouse brain PrP^C and PrP^{Sc}. We found partial and strong colocalizations of lysosomes and PrP^C and PrP^{Sc} on day 1, and almost all PrP^C and PrP^{Sc} particles were colocalized with lysosome on day 5 (Fig. 4A). These results suggest that lysosomes partially digest PrP^C and PrP^{Sc}.

4. Discussion

One prominent feature of TSEs is the absence of an adaptive host immune response. In the mouse scrapie model, however, the immune system is involved in either prion propagation or transmission. In the murine LRS, spleen and lymph nodes for example, are critical for PrP^{Sc} replication and neuroinvasion (Blatter et al., 1997; Mabbott et al., 2000). On the other hand, murine macrophages and dendritic cells (DCs) degrade TSE agents (Carp and Callahan, 1982; Rybner-Barnier et al., 2006), suggesting pathogenesis is based on their respective PrP^{Sc} formation in combination with intracellular degradation of PrP^{Sc} in mouse LRS. Although prion propagation sites and the roles of bovine immune cells remain to be determined, the distal ileum has been shown to accumulate PrP^{Sc} (Buschmann and Groschup, 2005).

Moreover, cattle experimentally inoculated by BSE-affected brain showed PrP^{Sc} localization in the follicles of the Peyer's patches, particularly in the macrophages (Terry et al., 2003). The roles of phagocytic cells that eliminate PrP^{Sc}, however, have not been thoroughly investigated. In our study, we used bovine phagocytic cells that combat exogenous pathogens and have shown strong degradation abilities against exogenous PrP^{Sc}. Our mouse scrapie PrP^{Sc} and bovine macrophage BSE degradation results concur with the mouse macrophage clearance reports of scrapie (Carp and Callahan, 1982) and BSE (Rybner-Barnier et al., 2006) *in vitro*, and of DCs in rat (Huang et al., 2002) and mouse (Luhr et al., 2002). Even though TSEs do not cause any inflammation, innate immunity must be utilized in order to prevent their respective diseases.

Our results also demonstrate the persistence of significant infectivity in cell cultures long after the disappearance of detectable PrP^{Sc}. We found that PrP^{Sc} is not detected within cell cultures 36 d following incubation with mouse scrapie brain homogenate by western blot analysis; and although infectivity still exists, confirming that this bioassay has superior sensitivity is necessary for evaluating infectivity. There are several hypotheses for PrP^{Sc} in infecting mouse brain homogenates after long degradation periods with macrophages *in vitro*: (1) PrP^{Sc} could be digested in small infectious peptides, which cannot be easily detected by western blot analysis and (2) some PrP^{Sc} attached onto cellular membranes or were exported to the supernatant following phagocytosis, and thus evade digestion. These situations may be similar to that *in vivo*, and the remaining infectivity shown in this study is an interesting topic for propagating disease in the individual host.

On the other hand, mouse inoculation assay results also demonstrate pathogenesis reduction of bovine macrophage degradation products. Bovine macrophages could reduce prion pathogeneses and might contribute to host protection. Under natural exposure PrP^{Sc} may enter the host through the ileum, and the macrophages in the ileum may act as the initial defender against PrP^{Sc}. The inoculums used in this study were at an extremely high titer compared to natural exposure concentrations. Under natural exposure situations macrophages are able to destroy the infectivity of PrP^{Sc} because the TSE infectivity is dose-dependent (Wells et al., 2007). Although information is limited, we hypothesize that small doses of infectivity by PrP^{Sc} may be easily destroyed by macrophages, whereas higher doses withstand complete destruction.

In BSE affected cattle, PrP^{Sc} was only found in CNS and not LRS, with the exception of the distal ileum (Buschmann and Groschup, 2005). Sheep orally infected with brain tissue from BSE cattle showed PrP^{Sc} accumulations in the lymph nodes, tonsil, and spleen, similar to sheep scrapie (Jeffrey et al., 2001). This differs from that of BSE in bovine. These data suggest that the prion disease feature is determined not by agent properties, but by host factors. The accumulation sites of PrP^{Sc} and infectivity in bovine differ from that in sheep, even though they are both ruminants. The bovine is supposed to have a unique system for both PrP^{Sc} propagating and clearance because of a species-specific difference, e.g., the immune system. This is the first study to define the use of bovine macrophages and degradation of PrP^{Sc} *in vitro* as a bovine-specific situation.

The PrP^{Sc} degradation by certain cells has been questioned. In mouse neuroblastoma 2a (N2a) cells are

persistently infected with prions, PrP^{C} and PrP^{Sc}, and destruction is thought to occur in the lysosome (Gilch et al., 2001). Treatment with PrP^{C} antibodies (Peretz et al., 2001) and peptidoglycans (Caughey and Raymond, 1993) could reduce PrP^{Sc}, thus implicating the existence of an intracellular PrP^{Sc} degradation pathway. In murine DC, colocalization of PrP^{Sc} and lysosome was reported (Luhr et al., 2004). These reports concur with our colocalization results of PrP^{Sc} and lysosomes. Phagocytosed materials are trapped in phagosome, which then fuse with a lysosome, and are digested by lysosomal enzymes. Further study on the PrP^{Sc} degradation pathway is necessary.

In conclusion, this study provides direct evidence that bovine macrophages can cause a progressive and efficient degradation of PrP^{Sc} in TSE brain homogenates. I recommend that cattle possess biological clearance systems such as innate immunity against prions, which may protect from infection with BSE.

Acknowledgements

We would like to thank Dr. M. Kodama (formally at the National Institute of Animal Health, Japan) for providing the Bo120 cell line, Dr. Mitsutaka Nakamura (Gifu Prefecture, Japan) for bovine blood, Dr. Tetsutaro Sata (National Institute of Infectious Diseases, Japan) for the brain homogenate of BSE Kanagawa case no. 10, and Dr. Motohiro Horiuchi (Hokkaido University, Japan) for providing mAb 31C6. This work was supported by a grant (17380180) from the Ministry of Education, Culture, Sports, Science, and Technology, and also by a grant from the Ministry of Health, Labour and Welfare of Japan.

References

Anderson, R.M., Donnelly, C.A., Ferguson, N.M., Woolhouse, M.E., Watt, C.J., Udy, H.J., MaWhinny, S., Dunstan, S.P., Southwood, T.R., Wilesmith, J.W., Ryan, J.B., Hoinville, L.J., Hillerton, J.E., Austin, A.R., Wells, G.A., 1996. Transmission dynamics and epidemiology of BSE in British cattle. Nature 382, 779–788.

Buschmann, A., Groschup, M.H., 2005. Highly bovine spongiform encephalopathy-sensitive transgenic mice confirm the essential restriction of infectivity to the nervous system in clinically diseased cattle. J. Infect. Dis. 192, 934–942.

Blatter, T., Brandner, S., Raeber, A.J., Klein, M.A., Voigtlander, T., Weissmann, C., Aguzzi, A., 1997. PrP-expressing tissue required for transfer of scrapie infectivity form spleen to brain. Nature 389, 69–73.

Caughey, B., Raymond, G.J., 1993. Sulfated polyanion inhibition of scrapie-associated PrP accumulation in cultured cells. J. Virol. 67, 643–650.

Carp, R.I., Callahan, S.M., 1982. Effect of mouse peritoneal macrophages on scrapie infectivity during extended in vitro incubation. Intervirology 17, 201–207.

Collinge, J., Sidle, K.C., Meads, J., Ironside, J., Hill, A.F., 1996. Molecular analysis of prion strain variation and the aetiology of 'new variant' CJD. Nature 383, 685–690.

Gilch, S., Winklhofer, K.F., Groschup, M.H., Nunziante, M., Lucassen, R., Spielhaupter, C., Muranyi, W., Riesner, D., Tatzelt, J., Schaetzl, H.M., 2001. Intracellular re-routing of prion protein prevents propagation of PrP^{Sc} and delays onset of prion disease. EMBO J. 20, 3957–3966.

Huang, F.P., Farquhar, C.F., Mabbott, N.A., Bruce, M.E., MacPherson, G.G., 2002. Migrating intestinal dendritic cells transport PrP^{Sc} from the gut. J. Gen. Virol. 83, 267–271.

Jeffrey, M., Ryder, S., Martin, S., Hawkins, S.A., Terry, L., Berthelin-Baker, C., Bellworthy, S.J., 2001. Oral inoculation of sheep with the agent of bovine spongiform encephalopathy (BSE). 1. Onset and distribution of disease-specific PrP accumulation in brain and viscera. J. Comp. Pathol. 124, 280–289.

Kim, C.L., Umetani, A., Matsui, T., Ishiguro, N., Shinagawa, M., Horiuchi, M., 2004a. Antigenic characterization of an abnormal isoform of prion protein using a new diverse panel of monoclonal antibodies. Virology 320, 40–51.

Kim, C.L., Karino, A., Ishiguro, N., Shinagawa, M., Sato, M., Horiuchi, M., 2004b. Cell-surface retention of PrP^{C} by anti-PrP antibody prevents protease-resistant PrP formation. J. Gen. Virol. 85, 3473–3482.

Luhr, K.M., Wallin, R.P., Ljunggren, H.G., Low, P., Taraboulos, A., Kristensson, K., 2002. Processing and degradation of exogenous prion protein by $CD11c^{+}$ myeloid dendritic cells in vitro. J. Virol. 76, 12259–12264.

Luhr, K.M., Nordstrom, E.K., Low, P., Ljunggren, H.G., Taraboulos, A., Kristensson, K., 2004. Scrapie protein degradation by cysteine proteases in $CD11c^{+}$ dendritic cells and GT1-1 neuronal cells. J. Virol. 78, 4776–4782.

Mabbott, N.A., Mackay, F., Minns, F., Bruce, M.E., 2000. Temporary inactivation of follicular dendritic cells delays neuroinvasion of scrapie. Nat. Med. 6, 719–720.

Maignien, T., Lasmezas, C.I., Beringue, V., Dormont, D., Deslys, J.P., 1999. Pathogenesis of the oral route of infection of mice with scrapie and bovine spongiform encephalopathy agents. J. Gen. Virol. 80, 3035–3042.

Montrasio, F., Frigg, R., Glatzel, M., Klein, M.A., Mackay, F., Aguzzi, A., Weissmann, C., 2000. Impaired prion replication in spleens of mice lacking functional follicular dendritic cells. Science 288, 1257–1259.

Peretz, D., Williamson, R.A., Kaneko, K., Vergara, J., Leclerc, E., Schmitt-Ulms, G., Mehlhorn, I.R., Legname, G., Wormald, M.R., Rudd, P.M., Dwek, R.A., Burton, D.R., Prusiner, S.B., 2001. Antibodies inhibit prion propagation and clear cell cultures of prion infectivity. Nature 412, 739–743.

Rybner-Barnier, C., Jacquemot, C., Cuche, C., Dore, G., Majlessi, L., Gabellec, M.M., Moris, A., Schwarts, O., Di Santo, J., Cumano, A., Leclerc, C., Lazarini, F., 2006. Processing of the bovine spongiform encephalopathy-specific prion protein by dendritic cells. J. Virol. 80, 4656–4663.

Shinagawa, M., Munekata, E., Doi, S., Takahashi, K., Goto, H., Sato, G., 1986. Immunoreactivity of a synthetic pentadecapeptide corresponding to the N-terminal region of the scrapie prion protein. J. Gen. Virol. 67, 1745–1750.

Sigurdson, C.J., Barillas-Mury, C., Miller, M.W., Oesch, B., van Keulen, L.J., Langeveld, J.P., Hoover, E.A., 2002. PrP^{CWD} lymphoid cell targets in early and advanced chronic wasting disease of mule deer. J. Gen. Virol. 83, 2617–2628.

Terry, L.A., Marsh, S., Ryder, S.J., Hawkins, S.A., Wells, G.A., Spencer, Y.I., 2003. Detection of disease-specific PrP in the distal ileum of cattle exposed orally to the agents of bovine spongiform encephalopathy. Vet. Rec. 152, 387–392.

van Keulen, L.J., Schreuder, B.E., Meloen, R.H., Mooij-Harkes, G., Vromans, M.E., Langeveld, J.P., 1996. Immunohistochemical detection of prion protein in lymphoid tissues of sheep with natural scrapie. J. Clin. Microbiol. 34, 1228–1231.

Wadsworth, J.D., Joiner, S., Hill, A.F., Campbell, T.A., Desbruslais, M., Luthert, P.J., Collinge, J., 2001. Tissue distribution of protease resistant prion protein in variant Creutzfeldt-Jakob disease using a highly sensitive immunoblotting assay. Lancet 358, 171–180.

Wells, G.A., Spiropoulos, J., Hawkins, S.A., Ryder, S.J., 2005. Pathogenesis of experimental bovine spongiform encephalopathy: preclinical infectivity in tonsil and observations on the distribution of lingual tonsil in slaughtered cattle. Vet. Rec. 156, 401–407.

Wells, G.A., Konold, T., Arnold, M.E., Austin, A.R., Hawkins, S.A., Stack, M., Simmons, M.M., Lee, Y.H., Gavier-Widen, D., Dawson, M., Wilesmith, J.W., 2007. Bovine spongiform encephalopathy: the effect of oral exposure dose on attack rate and incubation period in cattle. J. Gen. Virol. 88, 1363–1373.

JOURNAL OF VIROLOGY, Apr. 2010, p. 3230–3238 Vol. 84, No. 7
0022-538X/10/$12.00 doi:10.1128/JVI.02387-09

Experimental Verification of a Traceback Phenomenon in Prion Infection[▽]

Atsushi Kobayashi,[1] Nobuyuki Sakuma,[1] Yuichi Matsuura,[2] Shirou Mohri,[2] Adriano Aguzzi,[3] and Tetsuyuki Kitamoto[1]*

Division of CJD Science and Technology, Department of Prion Research, Tohoku University Graduate School of Medicine, 2-1 Seiryo-machi, Aoba-ku, Sendai 980-8575, Japan[1]; Prion Disease Research Center, National Institute of Animal Health, Tsukuba, Ibaraki 305-0856, Japan[2]; and Institute of Neuropathology, University Hospital Zurich, CH-8002 Zurich, Switzerland[3]

Received 12 November 2009/Accepted 5 January 2010

The clinicopathological phenotypes of sporadic Creutzfeldt-Jakob disease (sCJD) correlate with the allelotypes (M or V) of the polymorphic codon 129 of the human prion protein (PrP) gene and the electrophoretic mobility patterns of abnormal prion protein (PrP^{Sc}). Transmission of sCJD prions to mice expressing human PrP with a heterologous genotype (referred to as cross-sequence transmission) results in prolonged incubation periods. We previously reported that cross-sequence transmission can generate a new prion strain with unique transmissibility, designated a traceback phenomenon. To verify experimentally the traceback of sCJD-VV2 prions, we inoculated sCJD-VV2 prions into mice expressing human PrP with the 129M/M genotype. These 129M/M mice showed altered neuropathology and a novel PrP^{Sc} type after a long incubation period. We then passaged the brain homogenate from the 129M/M mouse inoculated with sCJD-VV2 prions into other 129M/M or 129V/V mice. Despite cross-sequence transmission, 129V/V mice were highly susceptible to these prions compared to the 129M/M mice. The neuropathology and PrP^{Sc} type of the 129V/V mice inoculated with the 129M/M mouse-passaged sCJD-VV2 prions were identical to those of the 129V/V mice inoculated with sCJD-VV2 prions. Moreover, we generated for the first time a type 2 PrP^{Sc}-specific antibody in addition to type 1 PrP^{Sc}-specific antibody and discovered that drastic changes in the PrP^{Sc} subpopulation underlie the traceback phenomenon. Here, we report the first direct evidence of the traceback in prion infection.

Creutzfeldt-Jakob disease (CJD) is a lethal transmissible neurodegenerative disease caused by an abnormal isoform of prion protein (PrP^{Sc}), which is converted from the normal cellular isoform (PrP^{C}) (1, 23). The genotype (M/M, M/V, or V/V, where M and V are allelotypes) at polymorphic codon 129 of the human prion protein (PrP) gene and the type (type 1 or type 2) of PrP^{Sc} in the brain are major determinants of the clinicopathological phenotypes of sporadic CJD (sCJD) (15–18). Type 1 and type 2 PrP^{Sc} are distinguishable according to the size of the proteinase K-resistant core of PrP^{Sc} (PrP^{res}) (21 and 19 kDa, respectively), reflecting differences in the proteinase K cleavage site (at residues 82 and 97, respectively) (15, 18). According to this molecular typing system, sCJD can be classified into six subgroups (MM1, MM2, MV1, MV2, VV1, or VV2).

The homology of the PrP genes between inoculated animals and the inoculum determines the susceptibility to prion infection. Transmission of sCJD prions to mice expressing human PrP with a nonhomologous genotype (referred to as cross-sequence transmission) results in a relatively long incubation period (10, 12). Meanwhile, the cross-sequence transmission can generate a new prion strain. Transmission of sCJD-VV2 prions to mice expressing human PrP with the 129M/M genotype generates unusual PrP^{res} intermediate in size between type 1 and type 2 (10). We have designated this unusual PrP^{res} with an upward size shift (Sh+) from the inoculated type 2 template MM[VV2]2^{Sh+} PrP^{res}, where the notation is of the following form: host genotype [type of inoculated prion] type of generated PrP^{res}.

Similar to the MM[VV2]2^{Sh+} PrP^{res}, the intermediate-sized PrP^{res} has been observed in the plaque-type of dura mater graft-associated CJD (p-dCJD) (10, 13). Furthermore, a transmission study using p-dCJD prions revealed that PrP-humanized mice with the 129V/V genotype were highly susceptible to p-dCJD prions despite cross-sequence transmission (10). In addition, these 129V/V mice inoculated with p-dCJD prions produced type 2 PrP^{res} (10). These findings suggest that p-dCJD could be caused by cross-sequence transmission of sCJD-VV2 prions to individuals with the 129M/M genotype. We have designated this phenomenon "traceback." The traceback phenomenon was discovered for the first time by a transmission study using variant CJD (vCJD) prions (2). Mice expressing bovine PrP were highly susceptible to vCJD prions because vCJD was caused by cross-sequence transmission of bovine spongiform encephalopathy prions to human. These findings suggest that a traceback study can be a powerful tool to identify the origin of prions (2, 10, 11). However, the traceback phenomenon has not been verified experimentally despite the abundant circumstantial evidence described above.

To verify the traceback of sCJD-VV2 prions, we inoculated sCJD-VV2 prions into PrP-humanized mice with the 129M/M genotype as an experimental model of p-dCJD. Thereafter, we inoculated these MM[VV2]2^{Sh+} prions into PrP-humanized mice with the 129M/M or 129V/V genotype and compared the incubation period, neuropathology, and the type of PrP^{res} in the brain. Here, we report the first direct evidence of the traceback in prion infection.

* Corresponding author. Mailing address: Division of CJD Science and Technology, Department of Prion Research, Tohoku University Graduate School of Medicine, 2-1 Seiryo-machi, Aoba-ku, Sendai 980-8575, Japan. Phone: 81 22 717 8143. Fax: 81 22 717 8148. E-mail: kitamoto@mail.tains.tohoku.ac.jp.

▽ Published ahead of print on 20 January 2010.

TABLE 1. Primers used for the amplification of truncated human PrP gene fragments

Primer function and name	Sequence
Amplification of C-terminal truncation fragment	
BamHI-23	5′-GGATCCAAGAAGCGCCCGAAGCCTGGAGGA-3′
89-XhoI	5′-CTCGAGTCACCAGCCACCACCATGAGGCTG-3′
90-XhoI	5′-CTCGAGTCAACCCCAGCCACCACCATGAGG-3′
91-XhoI	5′-CTCGAGTCATTGACCCCAGCCACCACCATG-3′
92-XhoI	5′-CTCGAGTCATCCTTGACCCCAGCCACCACC-3′
93-XhoI	5′-CTCGAGTCAACCTCCTTGACCCCAGCCACC-3′
94-XhoI	5′-CTCGAGTCAGCCACCTCCTTGACCCCAGCC-3′
95-XhoI	5′-CTCGAGTCAGGTGCCACCTCCTTGACCCCA-3′
96-XhoI	5′-CTCGAGTCAGTGGGTGCCACCTCCTTGACC-3′
Amplification of N-terminal truncation fragment	
BamHI-82	5′-CGTGGATCCGGACAGCCTCATGGTGGTGGCTGG-3′
BamHI-84	5′-CGTGGATCCCCTCATGGTGGTGGCTGGGGTCAA-3′
BamHI-86	5′-CGTGGATCCGGTGGTGGCTGGGGTCAAGGAGGT-3′
BamHI-88	5′-CGTGGATCCGGCTGGGGTCAAGGAGGTGGCACC-3′
BamHI-90	5′-CGTGGATCCGGTCAAGGAGGTGGCACCCACAGT-3′
BamHI-92	5′-CGTGGATCCGGAGGTGGCACCCACAGTCAGTGG-3′
BamHI-94	5′-CGTGGATCCGGCACCCACAGTCAGTGGAACAAG-3′
BamHI-97	5′-CGTGGATCCAGTCAGTGGAACAAGCCGAGTAAG-3′
230-XhoI	5′-CCGCTCGAGTCACGATCCTCTCTGGTAATAGGCCTG-3′

MATERIALS AND METHODS

Production of PrP^{res} type-specific polyclonal antibodies. A synthetic peptide corresponding to human PrP residues 82 to 98 was used as the immunogen for type 1 PrP^{res}-specific antibody Tohoku 1 because residues 82 to 96 were retained in type 1 PrP^{res} but not in type 2 PrP^{res} after proteinase K digestion (18). For type 2 PrP^{res}-specific antibody Tohoku 2, a short synthetic peptide corresponding human PrP residues 97 to 103 was used as the immunogen because the length of the immunogen peptide is critical for the production of proteolytic cleavage site-specific polyclonal antibodies (25, 26). Cysteine residues were added to the C terminus of each peptide, which was utilized for conjugation to bovine thyroglobulin via EMCS [*N*-(6-maleimidocaproyloxy)succinimide] (Dojin). For the initial injection, 100 μg of conjugate was emulsified in complete Freund's adjuvant and subcutaneously injected into rabbits. For the boosting injections, 100 μg of conjugate was emulsified in incomplete Freund's adjuvant and was subcutaneously injected on days 7, 21, 35, 49, 63, 84, and 91. At day 98, the rabbits were sacrificed, and serum was collected. Antibodies were purified by affinity chromatography using the immunogen peptides. Another type 1 PrP^{res}-specific monoclonal antibody, POM2, reacts with repeated octapeptide epitopes 59 to 65, 67 to 73, 75 to 81, and 83 to 89 of human and murine PrP (21, 22).

Production of knock-in mice and transgenic mice. The production of knock-in mice expressing human PrP with 129M/M (Ki-Hu129M/M mice) and Ki-Hu129V/V mice has been reported previously (2). Ki-Hu129M/M mice and knock-in mice expressing human PrP with 129M/M and four octapeptide repeats (Ki-Hu129M_{4R}/M_{4R}) were crossed with transgenic mice expressing human PrP with 129M (Tg-Hu129M) and four octapeptide repeats (Tg-Hu129M_{4R}), respectively (10). The expression levels of human PrP in the brains from Tg+Ki-Hu129M/M and Tg+Ki-Hu129M_{4R}/M_{4R} mice were 1.2-fold and 9.8-fold, respectively, the levels observed in Ki-Hu129M/M mice.

Human brain inocula. Brain tissues were obtained at autopsy from CJD patients after informed consent for research use was received. The diagnosis of CJD and the type of PrP^{Sc} were confirmed by neuropathological examination, PrP^{Sc} immunohistochemistry, and Western blotting as described previously (7, 27). The genotype and the absence of mutations in the open reading frame of the PrP gene were determined by sequence analysis (8). The CJD cases selected for the transmission studies were typical of the sCJD-MM1 and sCJD-VV2 subgroups. In the sCJD-VV2 (AK) isolate, the plaque-type PrP deposition in the brain and the absence of periodic synchronous discharges on electroencephalogram were confirmed. More detailed information of the patient was reported previously (4). Isolates sCJD-MM1 (H3) and sCJD-VV2 (AK) showed the same levels of transmissibility to PrP-humanized mice as other sCJD-MM1 and sCJD-VV2 isolates, respectively (27).

Transmission experiments. Human brain homogenates (10%) and mouse brain homogenates (10%) were prepared as described previously (9). Intracerebral transmission was performed using 20 μl of the homogenates (27). The inoculated mice were sacrificed after the onset of disease, and their brains were immediately frozen or fixed in 10% buffered formalin.

Immunohistochemistry. Formalin-fixed mouse brains were treated with 60% formic acid for 1 h to inactivate the infectivity and then were embedded in paraffin. Tissue sections were pretreated by hydrolytic autoclaving before PrP immunohistochemistry (7). The N-terminal PrP (PrP-N) antiserum was used as the primary antibody (6). Goat anti-rabbit immunoglobulin polyclonal antibody labeled with the peroxidase-conjugated dextran polymer EnVision+ (Dako-Cytomation) was used as the secondary antibody.

Expression of a GST-recombinant PrP fusion protein. The open reading frame of the human PrP gene was amplified by PCR with human DNA. The amplified fragment was cloned into pBluescript plasmid (Stratagene). With the plasmid construct, N-terminally or C-terminally truncated human PrP gene fragments were amplified by PCR. The primers used for the amplification are shown in Table 1. These primers introduced BamHI sites at the 5′ end of the fragments and XhoI sites at the 3′ end of the fragments. The amplified fragments were cloned into pGEM-T Easy plasmid (Promega). After digestion with BamHI and XhoI, the fragments were inserted into the BamHI/XhoI sites of the expression vector pGEX-4T-1 (GE Healthcare). *Escherichia coli* BL21(DE3) cells were transformed with the pGEX-4T-1 plasmid constructs, and recombinant PrP fragments fused to glutathione *S*-transferase (GST) were purified using glutathione Sepharose 4B beads (GE Healthcare) according to the manufacturer's instructions. GST-tagged recombinant PrP fragments were subjected to 13% SDS-PAGE and Western blotting.

Enzyme-linked immunosorbent assay (ELISA). Synthetic peptides corresponding to human PrP residues 97 to 103 and 93 to 103 were used as the antigens. Plates were individually coated with 50 ng/50 μl/well antigen or with 0.1% bovine serum albumin (BSA). The polyclonal antibody Tohoku 2 was serially diluted and added to each well as the primary antibody. A goat anti-rabbit IgG Fab′ fraction labeled with horseradish peroxidase was used as the secondary antibody. The color was developed with o-phenylenediamine.

Western blotting. PrP^{Sc} was extracted from mouse brains with collagenase treatment as described previously (5) with some modifications. Samples were subjected to 13% SDS-PAGE and Western blotting as described previously (2). The monoclonal antibody 3F4 (Signet Laboratories), PrP-N (Immuno-Biological Laboratories), C-terminal PrP ([PrP-C] Immuno-Biological Laboratories), POM2, Tohoku 1, and Tohoku 2 were used as the primary antibodies. Anti-mouse EnVision+ and anti-rabbit EnVision+ were used as the secondary antibodies. The signal intensities of the Western blots were quantified with Quantity One software using a VersaDoc 5000 (Bio-Rad Laboratories) imaging device.

Statistical analysis. Incubation times and signal intensities of PrP^{res} bands are expressed as mean ± standard error of the mean (SEM).

TABLE 2. Transmission of sCJD prions to humanized mice with the 129M/M or 129V/V genotype

Inoculum	Incubation period (days [mean ± SEM]) in the indicated mouse strain[a]		
	Tg+Ki-Hu129M/M (1.2×)[b]	Ki-Hu129M/M (1×)[b]	Ki-Hu129V/V (1×)[b]
sCJD-MM1 (H3)	429 ± 6 (6/6)	467 ± 24 (8/8)	774 ± 32 (6/6)
sCJD-VV2 (AK)	723 ± 79 (4/4)	633 ± 49 (6/6)	312 ± 7 (4/4)
MM[VV2]2^{Sh+}	ND	685 ± 17 (6/6)	309 ± 3 (7/7)

[a] Values in parentheses are the number of diseased animals/number of inoculated animals. ND, not done.
[b] The expression level of human PrP in the brain.

RESULTS

Transmission of MM[VV2]2^{Sh+} prions to PrP-humanized mice with the 129M/M or 129V/V genotype. To verify the traceback of sCJD-VV2 prions, we performed intracerebral inoculation of a brain homogenate from as sCJD-VV2 patient into Tg+Ki-Hu129M/M mice. Thereafter, we performed the second passage of the brain homogenate from a Tg+Ki-Hu129M/M mouse inoculated with sCJD-VV2 prions (MM[VV2]2^{Sh+} prions). Since Tg+Ki-Hu129M/M mice were established before the Ki-Hu129M/M mice were produced, we used them in the primary transmission of sCJD-VV2 prions. The data of the primary transmission have been reported previously (10). The mean incubation time of Tg+Ki-Hu129M/M mice inoculated with sCJD-VV2 prions was 723 ± 79 days (number of diseased animals/number of inoculated animals, 4/4) (Table 2). In the second passage, we inoculated MM[VV2]2^{Sh+} prions intracerebrally into Ki-Hu129M/M mice or Ki-Hu129V/V mice. Ki-Hu129M/M mice inoculated with MM[VV2]2^{Sh+} prions showed long incubation times of 685 ± 17 days (6/6). In contrast, the mean incubation time of Ki-Hu129V/V mice inoculated with MM[VV2]2^{Sh+} prions was shortened to 309 ± 3 days (7/7). In spite of cross-sequence transmission, the mean incubation time of Ki-Hu129V/V mice was much shorter than that of Ki-Hu129M/M mice. Immunohistochemical analysis of the brains from Tg+Ki-Hu129M/M mice inoculated with sCJD-VV2 prions showed large plaque-type PrP deposits spread throughout the cerebral gray matter and thalamus (Fig. 1). Ki-Hu129M/M mice inoculated with MM[VV2]2^{Sh+} prions showed similar patterns of PrP deposition to those of Tg+Ki-Hu129M/M mice inoculated with sCJD-VV2 prions. In contrast, Ki-Hu129V/V mice inoculated with MM[VV2]2^{Sh+} prions showed diffuse synaptic-type PrP deposits in the gray matter and small plaque-type deposits restricted to the cerebral white matter. These patterns of PrP deposition were identical to those of Ki-Hu129V/V mice inoculated with sCJD-VV2 prions. Thus, we confirmed that Ki-Hu129V/V mice were highly susceptible to MM[VV2]2^{Sh+} prions that originated from sCJD-VV2 prions and that the neuropathology of Ki-Hu129V/V mice inoculated with MM[VV2]2^{Sh+} prions was identical to that of the Ki-Hu129V/V mice inoculated with the parental sCJD-VV2 prions.

Characterization of PrP^{res} in the mouse brains using PrP^{res} type-specific antibodies. Tg+Ki-Hu129M/M mice inoculated with sCJD-VV2 prions produced unusual PrP^{res} with an upward size shift from the inoculated type 2 template (10). To characterize these type 2^{Sh+} PrP^{res}, we produced PrP^{res} type-specific antibodies. Type 1 PrP^{res}-specific polyclonal antibody Tohoku 1 reacted with epitopes located between residues 82 and 96 of human PrP (Fig. 2). Type 2 PrP^{res}-specific polyclonal antibody Tohoku 2 reacted with a synthetic peptide corresponding to human PrP residues 97 to 103 (the immunogen peptide) but not with the peptide at residues 93 to 103 (Fig. 3). The amino group at the N terminus of the immunogen peptide might constitute an essential part of the epitopes for Tohoku 2, as reported in other proteolytic cleavage site-specific antibodies (25, 26). Therefore, Tohoku 1 should specifically detect type 1 PrP^{res}, and Tohoku 2 should specifically detect the N-terminal cleavage site of type 2 PrP^{res} after proteinase K digestion (Fig. 4A).

First, with these PrP^{res} type-specific antibodies, we performed Western blot analysis of the PrP^{res} in the human brain inocula used in this transmission study (Fig. 4B). In addition to the newly generated type-specific antibodies, we used the monoclonal antibody POM2, which also specifically detects

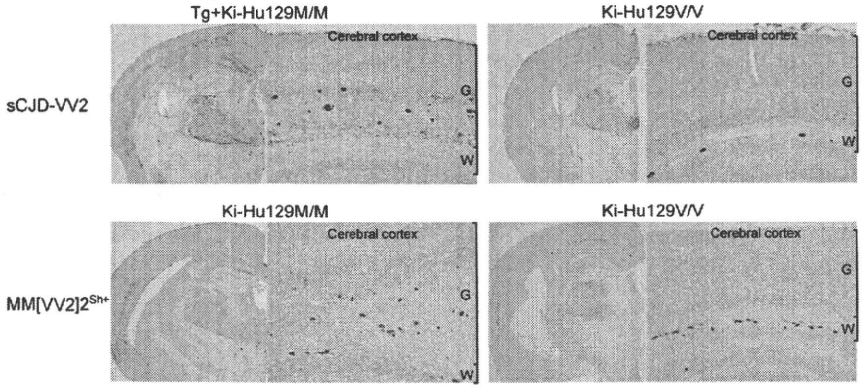

FIG. 1. The changes in neuropathology through cross-sequence transmission and traceback transmission. Immunohistochemical analysis of PrP^{Sc} in the brains from PrP-humanized mice inoculated with sCJD-VV2 prions or Tg+Ki-Hu129M/M mouse-passaged sCJD-VV2 prions. Tg+Ki-Hu129M/M mice inoculated with sCJD-VV2 prions or Ki-Hu129M/M mice inoculated with MM[VV2]2^{Sh+} prions showed prominent plaque-type PrP deposits throughout the cerebral gray matter. In contrast, plaque-type PrP deposits were restricted to within the white matter in the brains from Ki-Hu129V/V mice inoculated with sCJD-VV2 prions or MM[VV2]2^{Sh+} prions. G, gray matter; W, white matter.

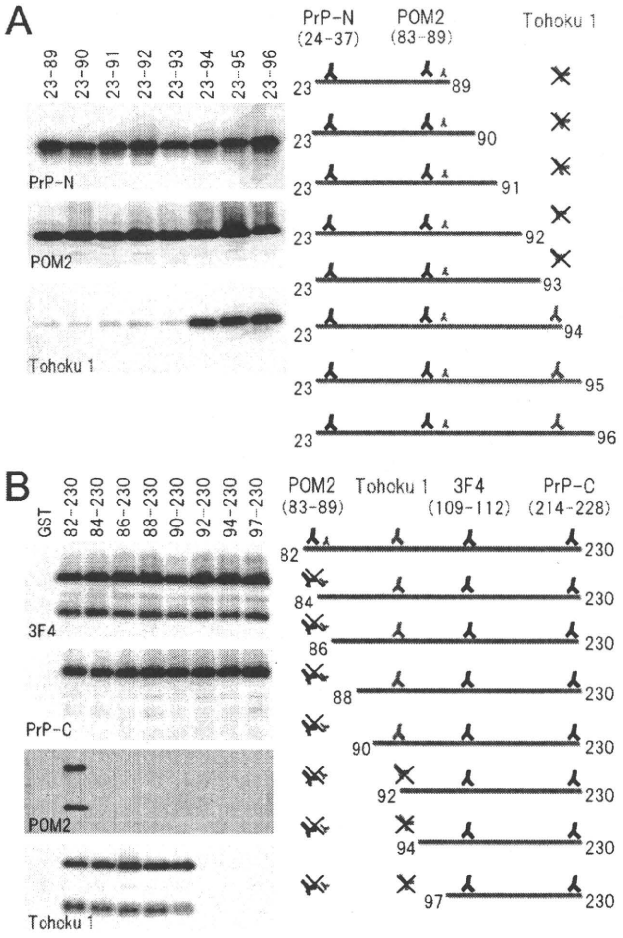

FIG. 2. Epitope mapping of polyclonal antibody Tohoku 1. (A) GST-tagged C-terminally truncated human PrP fragments were probed with PrP-N, POM2, or Tohoku 1. POM2 (21) reacted with all PrP fragments. In contrast, Tohoku 1 reacted with PrP fragments comprised of residues 23 to 94, 23 to 95, and 23 to 96. In addition, weak reactivity to PrP fragments 23 to 89, 23 to 90, 23 to 91, 23 to 92, and 23 to 93 was also observed. (B) GST-tagged N-terminally truncated human PrP fragments were probed with 3F4, PrP-C, POM2, or Tohoku 1. POM2 reacted with only the PrP fragment of residues 82 to 230. Tohoku 1 reacted with PrP fragments comprised of residues 82 to 230, 84 to 230, 86 to 230, 88 to 230, and 90 to 230. PrP residues 97 to 230, corresponding to proteinase K-digested type 2 PrP^{res} fragment, was not detected by Tohoku 1 or POM2. Low-molecular-weight bands lacking the PrP-C epitope should be degradation products. The reactivity of Tohoku 1 antibody (light blue), POM antibody (dark blue), and the other antibodies is summarized in a schematic diagram on the right.

type 1 PrP^{res} (Fig. 2) (21), as a reference antibody. Conventional typing of PrP^{res} using monoclonal antibody 3F4, which detects all PrP^{res} types, showed only a single PrP^{res} type in the brain of an sCJD-MM1 patient or in that of an sCJD-VV2 patient. With the PrP^{res} type-specific antibodies, however, small amounts of POM2/Tohoku 1-reactive subpopulations were observed in the sCJD-VV2 brain (Fig. 4B). The mean signal intensity of PrP^{res} in the sCJD-MM1 brain was assigned as 100/mm^2 in each experiment using 3F4, POM2, or Tohoku 1 (n = 3). In the Western blot analysis using 3F4, the mean signal intensity of PrP^{res} in the sCJD-VV2 brain was 224/mm^2 (Fig. 4B, white bars). In contrast, the signal intensities of POM2/Tohoku 1-reactive PrP^{res} bands in the sCJD-VV2 brain were 12/mm^2 (Fig. 4B, hatched bars) and 48/mm^2 (gray bars), respectively. Thus, using type 1 PrP^{res}-specific antibody, the sCJD-VV2 brain contained minority subpopulations that could be detected by type 1 PrP^{res}-specific antibodies, as reported previously (21, 28). The sizes of POM2/Tohoku 1-reactive bands were smaller than those of type 1 PrP^{res} in the sCJD-MM1 brain. Thus, POM2 and Tohoku 1 could detect the intermediate-sized PrP^{res} in addition to type 1 PrP^{res}. Furthermore, trace amounts of the Tohoku 2-reactive subpopulation were observed in the sCJD-MM1 brain (Fig. 4B, black bars). The mean signal intensity of PrP^{res} in the sCJD-VV2 brain was assigned as 100/mm^2 in each experiment using Tohoku 2 (n = 3). The mean signal intensity of Tohoku 2-reactive PrP^{res} bands in the sCJD-MM1 brain was 2/mm^2. Thus, using type 2 PrP^{res}-specific antibody, the minority type 2 PrP^{res} subpopulation could be detected even in the sCJD-MM1 brain.

Second, we performed Western blot analysis of PrP^{res} in the mouse brains using the PrP^{res} type-specific antibodies. Western blot analysis using 3F4 showed that Tg+Ki-Hu129M/M mice inoculated with sCJD-VV2 prions produced type 2^{Sh+} PrP^{res} that was located between type 1 PrP^{res} from Ki-Hu129M/M mice inoculated with sCJD-MM1 prions and type 2 PrP^{res} from Ki-Hu129V/V mice inoculated with sCJD-VV2 prions (Fig. 4C) (10). These PrP^{res} were probed with type-specific antibodies Tohoku 1, Tohoku 2, or POM2. The brains from Tg+Ki-Hu129M/M mice inoculated with sCJD-VV2 prions contained POM2/Tohoku 1-reactive PrP^{res} subpopulations in which the PrP^{res} were smaller than those of type 1 PrP^{res} from Ki-Hu129M/M inoculated with sCJD-MM1 prions. However, the signal intensities of these POM2/Tohoku 1-reactive bands were apparently decreased compared to those detected by 3F4 (Fig. 4C, bar graphs). The mean signal intensity of PrP^{res} from Ki-Hu129M/M mice inoculated with sCJD-MM1 prions was assigned as 100/mm^2 in each experiment using 3F4, POM2, or Tohoku 1 (n = 4). In the brains from Tg+Ki-Hu129M/M mice inoculated with sCJD-VV2 prions, the mean signal intensity of 3F4-reactive PrP^{res} bands was 154/mm^2 (white bars). However, the mean signal intensities of POM2/Tohoku 1-reactive PrP^{res} bands were 34/mm^2 (hatched bar) and 113/mm^2 (gray bar), respectively. Since more of the epitopes for Tohoku 1 were located at the C terminus than for POM2 (Fig. 2), the signal intensities of Tohoku 1-reactive bands might be higher than those of POM2-reactive bands. Thus, the brains from Tg+Ki-Hu129M/M mice inoculated with sCJD-VV2 prions contained the intermediate-sized PrP^{res}, but certain subpopulations that could not be detected by POM2 or Tohoku 1 must also have been present. The Tohoku 2-reactive subpopulation was not observed in Tg+Ki-Hu129M/M mice inoculated with sCJD-VV2 prions or Ki-Hu129M/M mice inoculated with sCJD-MM1 prions (Fig. 4C, black bars). The mean signal intensity of PrP^{res} from Ki-Hu129V/V mice inoculated with sCJD-VV2 prions was assigned as 100/mm^2 in each experiment using Tohoku 2 (n = 4). The brains from Ki-Hu129V/V mice inoculated with sCJD-VV2 prions contained small amounts of POM2/Tohoku 1-reactive subpopulations in addition to the Tohoku 2-reactive majority subpopulation. Thus, in the cross-sequence transmission of sCJD-VV2 prions to Tg+Ki-Hu129M/M mice, POM2/Tohoku 1-reactive subpopulations

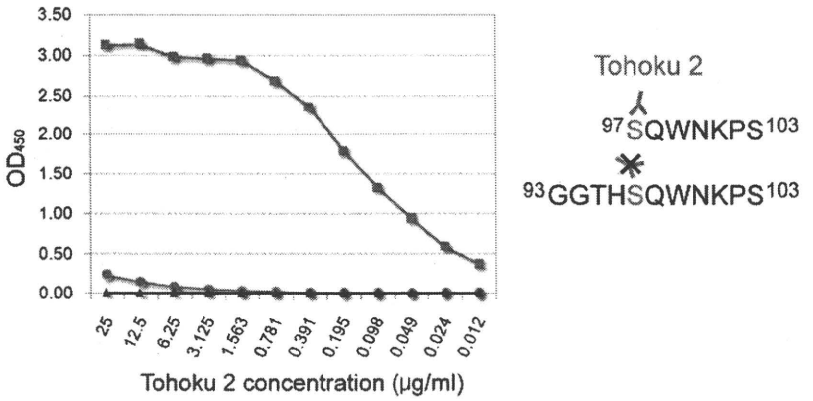

FIG. 3. Characterization of polyclonal antibody Tohoku 2 by peptide ELISA. Tohoku 2 specifically reacted with a synthetic peptide corresponding to human PrP residues 97 to 103 (■) but not with peptide at residues 93 to 103 (●). Control wells were coated with 0.1% BSA (▲). OD_{450}, optical density at 450 nm. The reactivity of Tohoku 2 antibody (pink) is summarized in a schematic diagram on the right. Tohoku 2 should recognize the N terminus of the human PrP fragment comprised of residues 97 to 103.

were increased, whereas the Tohoku 2 reactive-subpopulation was decreased. Therefore, the upward size shift from type 2 to type 2^{Sh+} in the Western blot analysis using 3F4 reflected the shift of the majority PrP^{res} subpopulation from the Tohoku 2-reactive subpopulation to the POM2/Tohoku 1-reactive subpopulation.

In the second passage of the brain homogenate from Tg+Ki-Hu129M/M mouse inoculated with sCJD-VV2 prions (MM[VV2]2^{Sh+} prions: host genotype [type of inoculated prions] type of generated PrP^{res}), Ki-Hu129M/M mice inoculated with MM[VV2]2^{Sh+} prions produced the intermediate-sized PrP^{res} that were identical in size to parental MM[VV2]2^{Sh+} prions when probed with 3F4 (Fig. 4C). Similar to the brains from Tg+Ki-Hu129M/M mice inoculated with sCJD-VV2 prions, the brains from Ki-Hu129M/M mice inoculated with MM[VV2]2^{Sh+} prions contained POM2/Tohoku 1-reactive subpopulations but not the Tohoku 2-reactive subpopulation. In the brains from Ki-Hu129M/M mice inoculated with MM[VV2]2^{Sh+} prions, the mean signal intensities of 3F4, POM2, and Tohoku 1-reactive PrP^{res} bands were 176/mm^2 (Fig. 4C, white bars), 85/mm^2 (hatched bars), and 139/mm^2 (gray bars), respectively. Meanwhile, Western blot analysis using 3F4 showed that Ki-Hu129V/V mice inoculated with MM[VV2]2^{Sh+} prions produced type 2 PrP^{res}; i.e., the intermediate-sized PrP^{res} reverted to type 2 when MM[VV2]2^{Sh+} prions were transmitted to Ki-Hu129V/V mice. Moreover, in the traceback transmission of MM[VV2]2^{Sh+} prions to Ki-Hu129V/V mice, POM2/Tohoku 1-reactive subpopulations were decreased, whereas the Tohoku 2 reactive-subpopulation predominated. In the brains from Ki-Hu129V/V mice inoculated with MM[VV2]2^{Sh+} prions, the mean signal intensities of 3F4, POM2, and Tohoku 1-reactive PrP^{res} bands were 179/mm^2 (Fig. 4C, white bars), 13/mm^2 (hatched bars), and 43/mm^2 (gray bars), respectively, whereas the mean signal intensity of the Tohoku 2-reactive PrP^{res} bands was 159/mm^2 (black bars). Thus, PrP^{res} type-specific antibodies revealed that cross-sequence transmission of sCJD-VV2 prions generated a new prion strain (MM[VV2]2^{Sh+} prions) with an altered proportion of PrP^{res} subpopulations and that the altered proportion reverted to the original proportion through the traceback transmission to Ki-Hu129V/V mice.

Traceback study of p-dCJD prions reevaluated with the PrP^{res} type-specific antibodies. We reported previously that p-dCJD prions showed the intermediate-sized PrP^{res}, and that Ki-Hu129V/V mice inoculated with p-dCJD prions showed accumulation of type 2 PrP^{res} (10). To characterize these PrP^{res} in the brains from PrP-humanized mice inoculated with p-dCJD prions, we performed Western blot analysis using PrP^{res} type-specific antibodies (Fig. 5). Since Tg+Ki-Hu129M_{4R}/M_{4R} mice were already established before the Ki-Hu129M/M mice were produced, we used them in the traceback study of p-dCJD or nonplaque-type dCJD (np-dCJD) prions. Subsequently, we confirmed that Tg+Ki-Hu129M_{4R}/M_{4R}, Ki-Hu129M/M, and Tg+Ki-Hu129M/M mice produced PrP^{res} identical in size in the transmission studies using various CJD prions (10). POM2/Tohoku 1-reactive subpopulations existed in the brains from Tg+Ki-Hu129M_{4R}/M_{4R} mice inoculated with p-dCJD prions, but the signal intensities were apparently decreased compared to those detected by 3F4 (Fig. 5). The mean signal intensity of PrP^{res} from Tg+Ki-Hu129M_{4R}/M_{4R} mice inoculated with sCJD-MM1 prions was assigned as 100/mm^2 in each experiment using 3F4, POM2, or Tohoku 1 (n = 3). In the brains from Tg+Ki-Hu129M_{4R}/M_{4R} mice inoculated with p-dCJD prions, the mean signal intensity of 3F4-reactive PrP^{res} bands was 105/mm^2 (Fig. 5, white bars). However, the mean signal intensities of POM2/Tohoku 1-reactive PrP^{res} bands were 23/mm^2 (hatched bars) and 45/mm^2 (gray bars), respectively. The POM2/Tohoku 1-reactive bands were smaller than those of type 1 PrP^{res} from Tg+Ki-Hu129M_{4R}/M_{4R} mice inoculated with np-dCJD prions or sCJD-MM1 prions. In addition, trace amounts of the Tohoku 2-reactive subpopulation were observed in the brains from Tg+Ki-Hu129M_{4R}/M_{4R} mice inoculated with p-dCJD prions, np-dCJD prions, or sCJD-MM1 prions (Fig. 5, black bars). The mean signal intensity of PrP^{res} from Ki-Hu129V/V mice inoculated with sCJD-VV2 prions was assigned as 100/mm^2 in each experiment using Tohoku 2 (n = 3). Since the sizes of these Tohoku 2-reactive bands were identical to those of

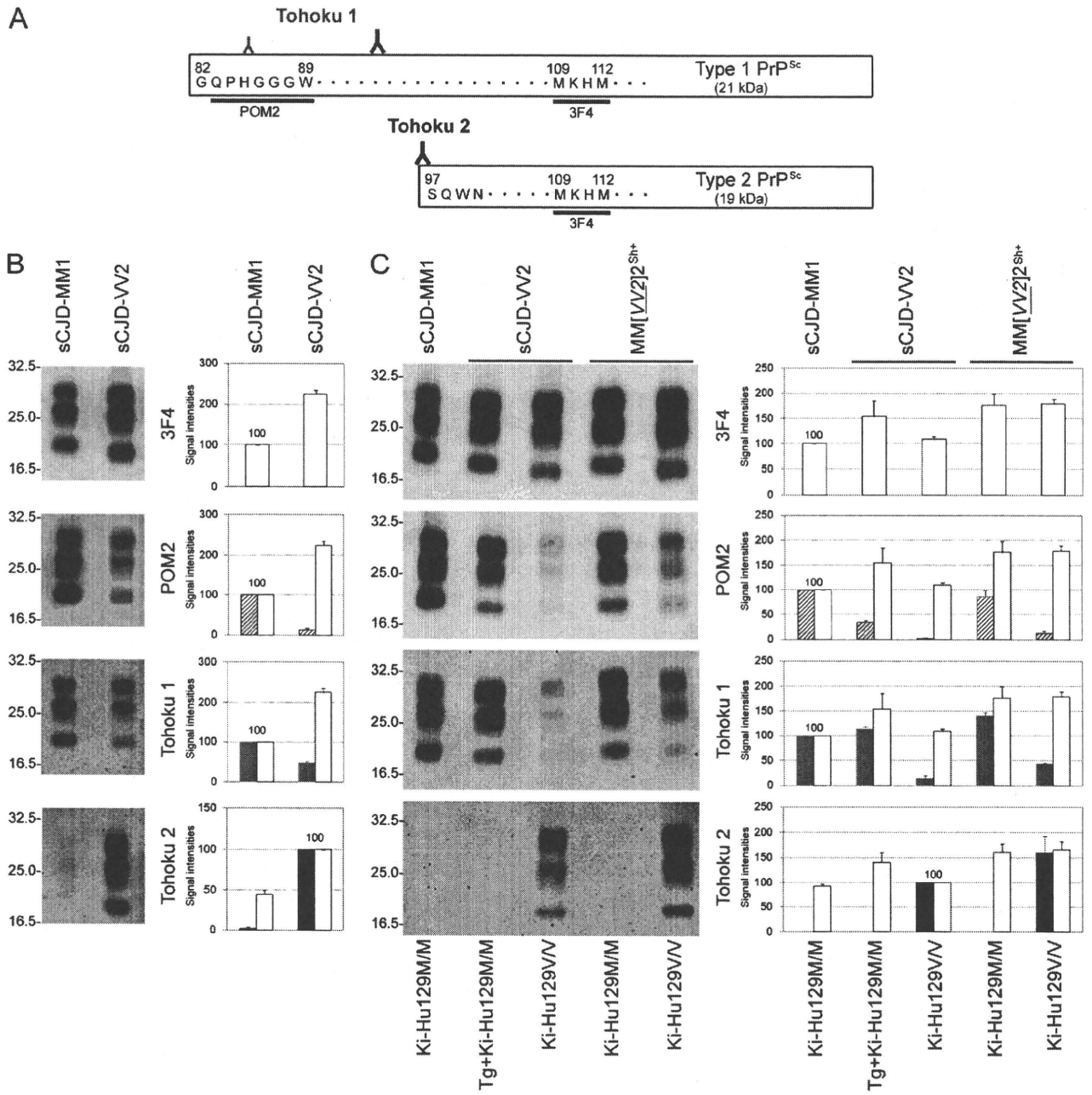

FIG. 4. Characterization of PrP^{res} using PrP^{res} type-specific antibodies. (A) The epitopes for type 1 PrP^{res}-specific polyclonal antibody Tohoku 1 (grey) or type 2 PrP^{res}-specific polyclonal antibody Tohoku 2 (black) are summarized in a schematic diagram. POM2 also specifically detects type 1 PrP^{res} (21). 3F4 detects all types of PrP^{res}. (B) Characterization of the human brain inocula used for the transmission studies. Western blot analysis using POM2 and Tohoku 1 revealed that the sCJD-VV2 brain contained minority subpopulations that could be detected by type 1 PrP^{res}-specific antibodies, as reported previously (21, 28). Meanwhile, using type 2 PrP^{res}-specific antibody Tohoku 2, the minority type 2 PrP^{res} subpopulation could be detected even in the sCJD-MM1 brain. The mean signal intensity of PrP^{res} in the sCJD-MM1 brain was assigned as 100/mm^2 in each experiment using 3F4 (white bars), POM2 (hatched bars), or Tohoku 1 (gray bars). The mean signal intensity of PrP^{res} in the sCJD-VV2 brain was assigned as 100/mm^2 in each experiment using Tohoku 2. The signal intensities of PrP^{res} are expressed as mean ± SEM (n = 3). (C) Western blot analysis using PrP^{res} type-specific antibodies revealed that drastic changes in the PrP^{res} subpopulations underlie the traceback phenomenon. In the cross-sequence transmission of sCJD-VV2 prions to Tg+Ki-Hu129M/M mice, POM2/Tohoku 1-reactive subpopulations were increased, whereas the Tohoku 2 reactive-subpopulation was decreased. Conversely, in the traceback transmission of $MM[VV2]2^{Sh+}$ prions to Ki-Hu129V/V mice, POM2/Tohoku 1-reactive subpopulations were decreased, whereas the Tohoku 2 reactive-subpopulation predominated. The signal intensity of PrP^{res} from Ki-Hu129M/M mice inoculated with sCJD-MM1 was assigned as 100/mm^2 in each experiment using 3F4 (white bars), POM2 (hatched bars), or Tohoku 1 (gray bars). The signal intensity of PrP^{res} from Ki-Hu129V/V mice inoculated with sCJD-VV2 was assigned as 100/mm^2 in each experiment using Tohoku 2 (black bars). The signal intensity of PrP^{res} is expressed as the mean ± SEM (n = 4).

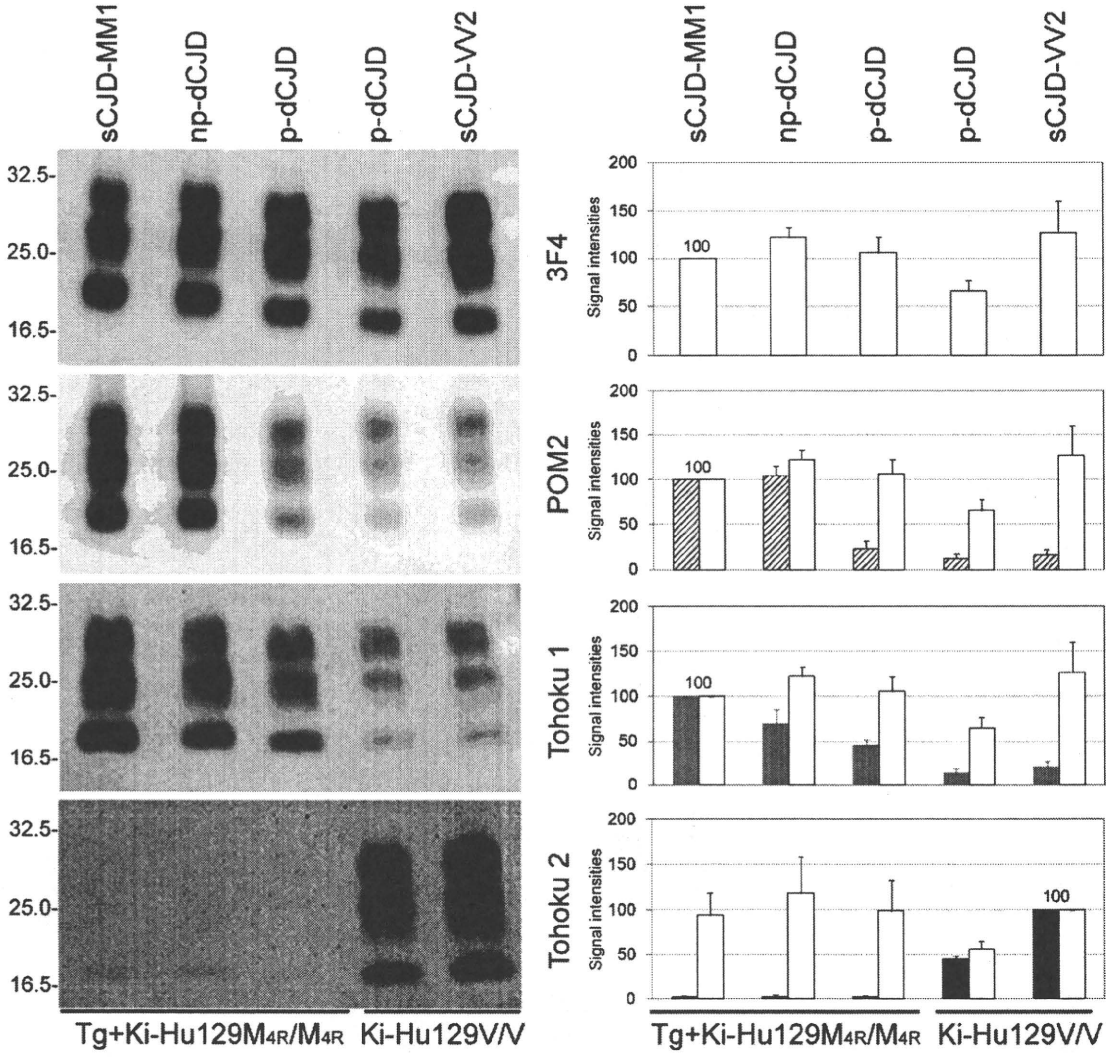

FIG. 5. Traceback study of p-dCJD prions reevaluated with PrP^{res} type-specific antibodies. In the traceback transmission of p-dCJD prions to Ki-Hu129V/V mice, POM2/Tohoku 1-reactive subpopulations were decreased, whereas the Tohoku 2 reactive-subpopulation predominated. In addition, trace amounts of the Tohoku 2-reactive subpopulation were observed in the brains from Tg+Ki-Hu129M_{4R}/M_{4R} mice inoculated with p-dCJD prions, np-dCJD prions, or sCJD-MM1 prions. The signal intensity of PrP^{res} from Tg+Ki-Hu129M_{4R}/M_{4R} mice inoculated with sCJD-MM1 was assigned as 100/mm^2 in each experiment using 3F4 (white bars), POM2 (hatched bars), or Tohoku 1 (gray bars). The signal intensity of PrP^{res} from Ki-Hu129V/V mice inoculated with sCJD-VV2 was assigned as 100/mm^2 in each experiment using Tohoku 2 (black bars). The signal intensity of PrP^{res} is expressed as the mean ± SEM (n = 3).

type 2 PrP^{res} from Ki-Hu129V/V mice inoculated with sCJD-VV2 prions, Tohoku 2 could specifically detect type 2 PrP^{res}. Meanwhile, in the transmission of p-dCJD prions to Ki-Hu129V/V mice, POM2/Tohoku 1-reactive subpopulations were decreased, whereas the Tohoku 2-reactive subpopulation predominated. In the brains from Ki-Hu129V/V mice inoculated with p-dCJD prions, the mean signal intensities of 3F4, POM2, and Tohoku 1-reactive PrP^{res} bands were 65/mm^2 (Fig. 5, white bars), 12/mm^2 (hatched bars), and 13/mm^2 (gray bars), respectively, whereas the mean signal intensity of Tohoku 2-reactive PrP^{res} bands was 45/mm^2 (black bars). Thus, the changes in PrP^{res} subpopulation observed in this traceback study of p-dCJD prions were identical to those observed in the traceback study of MM[VV2]2^{Sh+} prions.

DISCUSSION

In order to protect humans and animals from infectious diseases, it is often crucial to determine the origin of the isolates that may lie at the origin of epidemics. In the case of conventional pathogens, this is relatively simple and primarily involves the sequencing of pathogen-associated nucleic acids. Because prions lack informational nucleic acids, however, the unambiguous assignment of a given infection to a specific source is very often impossible. Therefore, methods aimed at characterizing stable prion properties after passaging through hosts would be extremely valuable.

Here, we demonstrate the first direct evidence of traceback in prion infection. Ki-Hu129V/V mice were highly susceptible

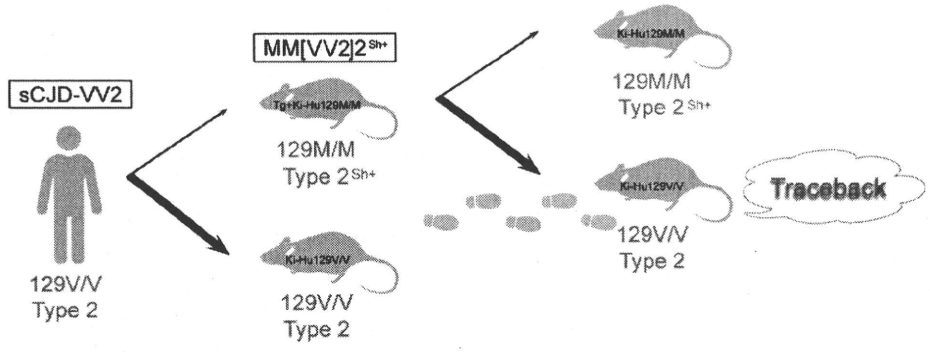

FIG. 6. Diagram of the traceback studies. The cross-sequence transmission of sCJD-VV2 prions to Tg+Ki-Hu129M/M mice generated a new prion strain (MM[VV2]2^{Sh+} prions) with altered conformational properties and disease phenotypes after a long incubation period. In the secondary transmission, Ki-Hu129V/V mice were highly susceptible to these MM[VV2]2^{Sh+} prions despite cross-sequence transmission. Furthermore, the altered conformational properties and disease phenotypes reverted to the original ones. If atypical prion strains emerge through cross-sequence transmission, traceback studies can be a reliable tool to identify the origin of prions.

to the Tg+Ki-Hu129M/M mouse-passaged sCJD-VV2 prions (MM[VV2]2^{Sh+} prions) despite cross-sequence transmission (Fig. 6). In addition, MM[VV2]2^{Sh+} prions and sCJD-VV2 prions exhibited similar neuropathologies and the identical PrP^{res} types when inoculated into Ki-Hu129V/V mice; i.e., the altered disease phenotypes and unusual PrP^{res} type of MM[VV2]2^{Sh+} prions reverted to those of the parental sCJD-VV2 prions. Furthermore, we generated for the first time type 2 PrP^{res}-specific polyclonal antibody Tohoku 2 in addition to type 1 PrP^{res}-specific polyclonal antibody Tohoku 1. These PrP^{res} type-specific antibodies revealed that drastic changes in the PrP^{res} subpopulations underlie the traceback phenomenon.

The present study clearly shows that traceback studies can be a reliable tool to identify the origin of prions if atypical prion strains emerge through cross-sequence transmission. Although the numbers of animals and human brain inocula used for the transmission were limited in the present study, we demonstrated experimentally the traceback phenomenon: Ki-Hu129V/V mice were highly susceptible to MM[VV2]2^{Sh+} prions that originated from sCJD-VV2 prions. In the cross-sequence transmission of sCJD-VV2 prions to Tg+Ki-Hu129M/M mice, POM2/Tohoku 1-reactive subpopulations were increased, whereas the Tohoku 2-reactive subpopulation was decreased. In contrast, the altered proportion of PrP^{res} subpopulations reverted to the original proportion through the traceback transmission to Ki-Hu129V/V mice. Similar changes in the PrP^{res} subpopulations were observed in the traceback transmission of p-dCJD prions to Ki-Hu129V/V mice. Therefore, the present study shows again that p-dCJD could be caused by cross-sequence transmission of sCJD-VV2 prions to individuals with the 129M/M genotype.

The drastic changes in the PrP^{res} subpopulations can be the molecular basis of the traceback phenomena. We suppose that the subpopulation change observed in the cross-sequence transmission is due to adaptation and/or a selection process (3, 20), which requires a relatively long incubation period. In contrast, the subpopulation change observed in the traceback transmission might be due to reemergence of the parental prions. Since the emerging prion strain generated by the cross-sequence transmission retains the memory of the parental prions within its conformational properties or repertoire of PrP^{Sc} subpopulations, the parental PrP^{Sc} subpopulation reemerges and becomes predominant if the emerging prion strain is transmitted to the original host. Therefore, the incubation period can be shortened, and the altered disease phenotypes revert to the original ones in traceback transmission.

Unexpectedly, type 2 PrP^{res}-specific antibody Tohoku 2 revealed that trace amounts of type 2 PrP^{res} coexisted with type 1 PrP^{res} in the brain of an sCJD-MM1 patient. In addition, PrP-humanized mice with the 129M/M genotype inoculated with sCJD-MM1 prions could produce trace amounts of type 2 PrP^{res} in addition to type 1 PrP^{res}. The additional type 2 PrP^{res} was detected in Tg+Ki-Hu129M_{4R}/M_{4R} but not in Ki-Hu129M/M mice. Since Tg+Ki-Hu129M_{4R}/M_{4R} mice express human PrP with four octapeptide repeats at 9.8-fold the level observed in Ki-Hu129M/M mice, these differences might account for the subtle change. Further large-scale studies are needed to determine whether an additional type 2 PrP^{res} can be detected by Tohoku 2 in other human CJD cases formerly classified as type 1.

The present study raises the possibility that cooccurrence of multiple PrP^{res} subpopulations in the same brain might be a general phenomenon. Both type 1 and type 2 PrP^{res} can be detected in the same brain in 35% of sCJD patients examined (19, 24). By using type 1 PrP^{res}-specific antibodies, the minority type 1 subpopulation can be detected with type 2 in all sCJD patients or variant CJD patients formerly classified as type 2 (21, 28). In accord with these reports, small amounts of type 1 (and the intermediate-sized) PrP^{res} were detected by type 1 PrP^{res}-specific antibodies in Ki-Hu129V/V mice inoculated with sCJD-VV2 prions in the present study. In addition, trace amounts of type 2 PrP^{res} were detected by type 2 PrP^{res}-specific antibody in the sCJD-MM1 patient or Tg+Ki-Hu129M_{4R}/M_{4R} mice inoculated with sCJD-MM1 prions. These findings are in line with a report that diverse PrP^{res} fragments can be detected by N-terminal amino acid sequencing in the same brain even though only a single PrP^{res} type is detected by conventional Western blot analysis (18). Since the conventional Western blot analysis using antibodies that react with all PrP^{res} types failed to detect type 1 PrP^{res} unless type 1 PrP^{res} represented more than 30 to 40% of total PrP^{res} in experimentally mixed

type 1 and type 2 brain samples, the cooccurrence of multiple PrP^{res} subpopulations might be underestimated (21, 28). Therefore, the "type" of PrP^{Sc} determined by the conventional typing system might merely represent the predominant PrP^{res} subpopulation among multiple subpopulations.

However, the biological importance of the minority PrP^{res} subpopulation detected by the PrP^{res} type-specific antibodies or by N-terminal amino acid sequencing remains to be determined. Insufficient proteinase K digestion can generate type 1-specific antibody-reactive PrP bands in brain samples from sCJD or vCJD patients classified as type 2 (14). Otherwise, the size of the PrP^{res} fragment might not always reflect the conformation of PrP^{Sc}; e.g., the minority MM1 PrP^{res} subpopulation detected in sCJD-MM2 patients might differ from the genuine MM1 PrP^{res} of sCJD-MM1 patients. It remains unknown whether the minority PrP^{res} subpopulation has infectivity and pathogenicity to cause prion disease. A concise and attractive explanation would be that the proportion of PrP^{Sc} subpopulations in the brain determines the disease phenotype, transmissibility, and the type of PrP^{Sc} determined by the conventional typing system, but further studies are needed to elucidate why multiple PrP^{res} subpopulations can be detected in the same brain. Therefore, the significance of the conventional molecular typing system using antibodies that react with all PrP^{res} types is likely to continue to be used in the classification of sCJD.

In conclusion, we verified experimentally that traceback studies can be a reliable tool to identify the origin of prions. The present study shows that the changes in PrP^{res} subpopulations correlate with the changes in prion strain-specific properties, e.g., transmissibility and disease phenotypes, in the traceback transmission. Hereafter, the proportion of PrP^{res} subpopulations in human CJD cases should be analyzed quantitatively using the PrP^{res} type-specific antibodies Tohoku 1 and Tohoku 2.

ACKNOWLEDGMENTS

We thank Y. Ishikawa, H. Kudo and K. Abe for excellent technical assistance and B. Bell for critical review of the manuscript.

This study was supported by the Program for Promotion of Fundamental Studies in Health Sciences of National Institute of Biomedical Innovation (S.M. and T.K.), a Grant-in-Aid from the Ministry of Health, Labor and Welfare (A.K., S.M., and T.K.), and a Grant-in-Aid for Scientific Research from the Ministry of Education, Culture, Sports, Science and Technology (A.K. and T.K.).

REFERENCES

1. **Aguzzi, A., and A. M. Calella.** 2009. Prions: protein aggregation and infectious diseases. Physiol. Rev. **89**:1105–1152.
2. **Asano, M., S. Mohri, J. W. Ironside, M. Ito, N. Tamaoki, and T. Kitamoto.** 2006. vCJD prion acquires altered virulence through trans-species infection. Biochem. Biophys. Res. Commun. **342**:293–299.
3. **Collinge, J., and M. R. Scott.** 2007. A general model of prion strains and their pathogenicity. Science **318**:930–936.
4. **Fukushima, R., Y. Shiga, M. Nakamura, J. Fujimori, T. Kitamoto, and Y. Yoshida.** 2004. MRI characteristics of sporadic CJD with valine homozygosity at codon 129 of the prion protein gene and PrP^{Sc} type 2 in Japan. J. Neurol. Neurosurg. Psychiatry **75**:485–487.
5. **Grathwohl, K. U. D., M. Horiuchi, N. Ishiguro, and M. Shinagawa.** 1996. Improvement of PrP^{Sc}-detection in mouse spleen early at the preclinical stage of scrapie with collagenase-completed tissue homogenization and Sarkosyl-NaCl extraction of PrP^{Sc}. Arch. Virol. **141**:1863–1874.
6. **Kitamoto, T., T. Muramoto, C. Hilbich, K. Beyreuther, and J. Tateishi.** 1991. N-terminal sequence of prion protein is also integrated into kuru plaques in patients with Gerstmann-Sträussler syndrome. Brain Res. **545**:319–321.
7. **Kitamoto, T., R. W. Shin, K. Doh-ura, N. Tomokane, M. Miyazono, T. Muramoto, and J. Tateishi.** 1992. Abnormal isoform of prion proteins accumulates in the synaptic structures of the central nervous system in patients with Creutzfeldt-Jakob disease. Am. J. Pathol. **140**:1285–1294.
8. **Kitamoto, T., M. Ohta, K. Doh-ura, S. Hitoshi, Y. Terao, and J. Tateishi.** 1993. Novel missense variants of prion protein in Creutzfeldt-Jakob disease or Gerstmann-Sträussler syndrome. Biochem. Biophys. Res. Commun. **191**: 709–714.
9. **Kitamoto, T., S. Mohri, J. W. Ironside, I. Miyoshi, T. Tanaka, N. Kitamoto, S. Itohara, N. Kasai, M. Katsuki, J. Higuchi, T. Muramoto, and R. W. Shin.** 2002. Follicular dendritic cell of the knock-in mouse provides a new bioassay for human prions. Biochem. Biophys. Res. Commun. **294**:280–286.
10. **Kobayashi, A., M. Asano, S. Mohri, and T. Kitamoto.** 2007. Cross-sequence transmission of sporadic Creutzfeldt-Jakob disease creates a new prion strain. J. Biol. Chem. **282**:30022–30028.
11. **Kobayashi, A., M. Asano, S. Mohri, and T. Kitamoto.** 2009. A traceback phenomenon can reveal the origin of prion infection. Neuropathology **29**: 619–624.
12. **Korth, C., K. Kaneko, D. Groth, N. Heye, G. Telling, J. Mastrianni, P. Parchi, P. Gambetti, R. Will, J. Ironside, C. Heinrich, P. Tremblay, S. J. DeArmond, and S. B. Prusiner.** 2003. Abbreviated incubation times for human prions in mice expressing a chimeric mouse-human prion protein transgene. Proc. Natl. Acad. Sci. U. S. A. **100**:4784–4789.
13. **Kretzschmar, H. A., S. Sethi, Z. Földvári, O. Windl, V. Querner, I. Zerr, and S. Poser.** 2003. Iatrogenic Creutzfeldt-Jakob disease with florid plaques. Brain Pathol. **13**:245–249.
14. **Notari, S., S. Capellari, J. Langeveld, A. Giese, R. Strammiello, P. Gambetti, H. A. Kretzschmar, and P. Parchi.** 2007. A refined method for molecular typing reveals that co-occurrence of PrP^{Sc} types in Creutzfeldt-Jakob disease is not the rule. Lab. Invest. **87**:1103–1112.
15. **Parchi, P., R. Castellani, S. Capellari, B. Ghetti, K. Young, S. G. Chen, M. Farlow, D. W. Dickson, A. A. F. Sima, J. Q. Trojanowski, R. B. Petersen, and P. Gambetti.** 1996. Molecular basis of phenotypic variability in sporadic Creutzfeldt-Jakob disease. Ann. Neurol. **39**:767–778.
16. **Parchi, P., S. Capellari, S. G. Chen, R. B. Petersen, P. Gambetti, N. Kopp, P. Brown, T. Kitamoto, J. Tateishi, A. Giese, and H. Kretzschmar.** 1997. Typing prion isoforms. Nature **386**:232–234.
17. **Parchi, P., A. Giese, S. Capellari, P. Brown, W. Schulz-Schaeffer, O. Windl, I. Zerr, H. Budka, N. Kopp, P. Piccardo, S. Poser, A. Rojiani, N. Streichemberger, J. Julien, C. Vital, B. Ghetti, P. Gambetti, and H. Kretzschmar.** 1999. Classification of sporadic Creutzfeldt-Jakob disease based on molecular and phenotypic analysis of 300 subjects. Ann. Neurol. **46**:224–233.
18. **Parchi, P., W. Zou, W. Wang, P. Brown, S. Capellari, B. Ghetti, N. Kopp, W. J. Schulz-Schaeffer, H. A. Kretzschmar, M. W. Head, J. W. Ironside, P. Gambetti, and S. G. Chen.** 2000. Genetic influence on the structural variations of the abnormal prion protein. Proc. Natl. Acad. Sci. U. S. A. **97**:10168–10172.
19. **Parchi, P., R. Strammiello, S. Notari, A. Giese, J. P. M. Langeveld, A. Ladogana, I. Zerr, F. Roncaroli, P. Cras, B. Ghetti, M. Pocchiari, H. Kretzschmar, and S. Capellari.** 29 August 2009. Incidence and spectrum of sporadic Creutzfeldt-Jakob disease variants with mixed phenotype and co-occurrence of PrP^{Sc} types: an updated classification. Acta Neuropathol. doi:10.1007/s00401-009-0585-1.
20. **Peretz, D., R. A. Williamson, G. Legname, Y. Matsunaga, J. Vergara, D. R. Burton, S. J. DeArmond, S. B. Prusiner, and M. R. Scott.** 2002. A change in the conformation of prions accompanies the emergence of a new prion strain. Neuron **34**:921–932.
21. **Polymenidou, M., K. Stoeck, M. Glatzel, M. Vey, A. Bellon, and A. Aguzzi.** 2005. Coexistence of multiple PrPSc types in individuals with Creutzfeldt-Jakob disease. Lancet Neurol. **4**:805–814.
22. **Polymenidou, M., R. Moos, M. Scott, C. Sigurdson, Y. Z. Shi, B. Yajima, I. Hafner-Bratkovic, R. Jerala, S. Hornemann, K. Wuthrich, A. Bellon, M. Vey, G. Garen, M. N. James, N. Kav, and A. Aguzzi.** 2008. The POM monoclonals: a comprehensive set of antibodies to non-overlapping prion protein epitopes. PLoS One **3**:e3872.
23. **Prusiner, S. B., M. R. Scott, J. P. DeArmond, and F. E. Cohen.** 1998. Prion protein biology. Cell **93**:337–348.
24. **Puoti, G., G. Giaccone, G. Rossi, B. Canciani, O. Bugiani, and F. Tagliavini.** 1999. Sporadic Creutzfeldt-Jakob disease: co-occurrence of different types of PrP^{Sc} in the same brain. Neurology **53**:2173–2176.
25. **Saido, T. C., S. Nagao, M. Shiramine, M. Tsukaguchi, H. Sorimachi, H. Murofushi, T. Tsuchiya, H. Ito, and K. Suzuki.** 1992. Autolytic transition of μ-calpain upon activation as resolved by antibodies distinguishing between the pre- and post-autolysis forms. J. Biochem. **111**:81–86.
26. **Saido, T. C., T. Iwatsubo, D. M. A. Mann, H. Shimada, Y. Ihara, and S. Kawashima.** 1995. Dominant and differential deposition of distinct β-amyloid peptide species, $A\beta_{N3(pE)}$, in senile plaques. Neuron **14**:457–466.
27. **Taguchi, Y., S. Mohri, J. W. Ironside, T. Muramoto, and T. Kitamoto.** 2003. Humanized knock-in mice expressing chimeric prion protein showed varied susceptibility to different human prions. Am. J. Pathol. **163**:2585–2593.
28. **Yull, H. M., D. L. Ritchie, J. P. M. Langeveld, F. G. van Zijderveld, M. E. Bruce, J. W. Ironside, and M. W. Head.** 2006. Detection of type 1 prion protein in variant Creutzfeldt-Jakob disease. Am. J. Pathol. **168**:151–157.